약학박사 학위논문

In situ real-time monitoring of methicillin-resistant Staphylococcus aureus biofilm formation using Raman spectroscopy

라만 분광학을 이용한 메틸실린 내성 포도상구균 바이오필름 성장 실시간 모니터링 연구

2023년 8 월

서울대학교 대학원

약학과 생약학전공

김 지 나

In situ real-time monitoring of methicillin-resistant Staphylococcus aureus biofilm formation using Raman spectroscopy

라만 분광학을 이용한 메틸실린 내성 포도상구균 바이오필름 성장 실시간 모니터링 연구

지도교수 진 영 원

이 논문을 약학박사 학위논문으로 제출함

2023년 7 월

서울대학교 대학원

약학과 생약학전공

김 지 나

김지나의 박사 학위논문을 인준함

2023년 8 월

위 원 장 _____ (인)

부위원장 _____ (인)

위 원 _____ (인)

위 원 _____ (인)

위 원 _____ (인)

Abstract

In situ real-time monitoring of methicillin-resistant Staphylococcus aureus biofilm formation using Raman spectroscopy

서울대학교
약학과 생약학전공
김지나

Recently, the prevalence of antimicrobial-resistant bacteria has been a critical challenge worldwide. Among the leading causes of infections is methicillin-resistant Staphylococcus aureus (MRSA), which forms biofilms on polymeric medical devices and implants, increasing their resistance to antibiotics by 10 - 1,000-fold. It is critical to apply antibiotics before biofilm formation. To diagnose early stage MRSA biofilm formation, the Raman spectrum was measured from 0 h to 48 h. Biofilms of MRSA were cultivated and characterized on a newly developed brain heart infusion-sucrose agar platform using Raman spectroscopy. Biofilm formation could be monitored by measuring DNA/RNA-associated Raman peaks and protein/lipid-associated peaks. During the first 5 h of incubation, monosaccharides, the main ingredient of the medium, produced Raman signals at 495 cm^{-1}. After

6 - 24 hours, 764, 1012, 1159, and 1526 cm^{-1} peaks correlated to DNA/RNA and carotenoids of biofilm increased, resulting in bacterial attachment and proliferation. During the 25 - 48 h of incubation, DNA/RNA-related signals decreased, and 1440 - 1460 cm^{-1} and 1630 cm^{-1} increased, reflecting the changes in lipids and proteins related to biofilm extracellular polymeric substances. Based on extensive Raman data, principal component analysis (PCA) classified three different stages of biofilm formation. Microscopy and the quantification of biofilm growth hourly confirmed early stage biofilm growth between 5 and 10 h of incubation time. To find the best time to efficiently eradicate MRSA biofilms, the antibacterial efficacy of Eugenol was applied at different hours. The monitored Raman spectrum showed that the most antibiotic susceptible time was found at the first 5 h of biofilm formation. Raman spectroscopy results were in good agreement with that from colony forming unit statistical analysis. According to these results, Raman spectroscopy can monitor biofilm formation in situ on solid culture medium and carry out rapid anti-biofilm tests by newly discovered antibiotics at the early stage of the process.

Keyword : Raman spectroscopy; Methicillin-resistant *Staphylococcus aureus*; Biofilm; Bacteria identification; Eugenol; Modified agar plate

Student Number : 2014-31243

Table of Contents

List of Schemes

List of Tables

List of Figures

List of Abbreviations

ANOVA	Analysis of variance
BHI	Brain heart infusion
CFU	Colony forming unit
CRA	Congo red assay
E. Coli	Escherichia coli
EPS	Extracellular polymeric substances
MBIC	Minimum biofilm inhibition concentration
MBHIA	Modified brain heart infusion agar
MIC	Minimum inhibitory concentrations
MRSA	Methicillin-resistant Staphylococcus aureus
OD	Optical density
PBS	Phosphate-buffered saline
PC	Principal component
PCA	Principal component analysis
PLS-DA	Partial Least-Squares Discriminant Analysis
SERS	Surface enhanced Raman scattering
TSA	Tryptic soy agar
TSB	Tryptic soy broth
ZOE	Zinc oxide-eugenol

Chapter 1. Introduction

1.1 Study Background

Infections caused by Staphylococcus aureus have emerged as one of the most significant global health problems. Various refractory infections are caused by S. aureus, primarily due to its ability to develop resistance to many drugs and form biofilm.
Methicillin-resistant S. aureus (MRSA) is among the most dreadful clinical diseases. Every year, 20 - 50 new cases are diagnosed for every 100,000 people, resulting in a mortality rate of 40% (Abbanat et al. 2014). The emergence of antibiotic resistant strains and their ability to form biofilms present a serious threat to modern medicine (Kranjec et al. 2020). When the right antibiotic is identified in an effective time frame, thousands of lives could be saved, and drug-resistant bacteria would be slowed down (Stöckel et al. 2016). Hence, the search for antibiotic treatment for drug-resistant bacteria and the exploration of MRSA biofilm is crucial (Wickramasinghe et al. 2020).

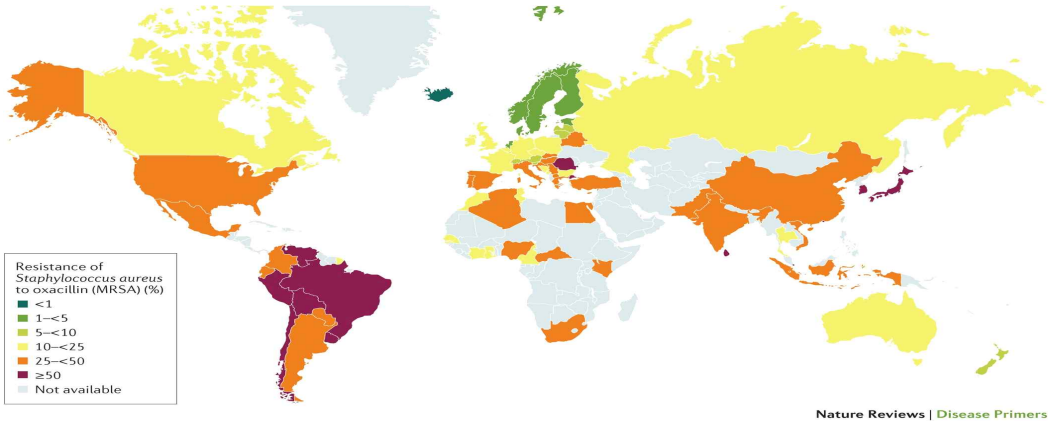

Figure 1. Worldwide prevalence of MRSA (Lee et al. 2018)

Biofilms are forms of microorganisms attached to extracellular polymeric substances (EPS) that provide a home to bacterial cells. Antibiotic-resistant cells develop into biofilms due to harsh environments, such as a lack of oxygen and insufficient nutrients. In this extreme condition, EPS gives stability and a niche to microorganisms. It is mainly composed of polysaccharides, proteins, lipids, and extracellular DNA (Verma et al. 2021). Biofilm formation involves complex developmental stages and usually follows three major phases: attachment, biofilm proliferation or maturation, and biofilm detachment or dispersal (O'Toole et al. 2000; Sauer et al. 2002). Since biofilms undergo remodeling by attaching to a surface, shedding planktonic bacteria, and organism proliferation, the matrix strengthens (Verma et al. 2021). Due to intense multicellular conglomerates, biofilms require up to 1000 times higher doses of antibiotics than planktonic bacteria (Smith 2005).

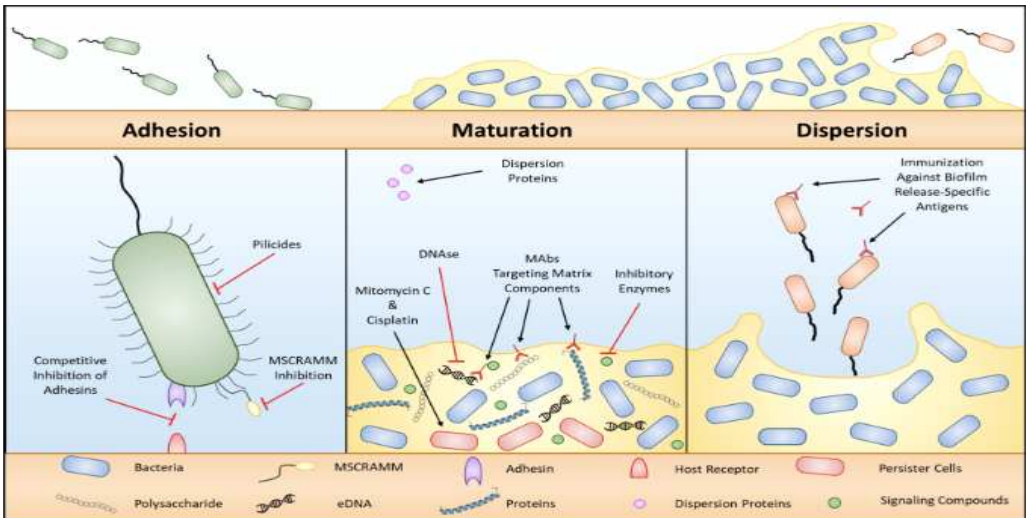

Figure 2. Biofilm generalized three phases: adhesion, maturation, and dispersion

Since biofilm infections are difficult to treat, rapid and easy diagnostic techniques are required to identify biofilm-forming S. aureus (Pebdeni et al. 2020). Traditionally, biofilms are identified by applying crystal violet dye, and their optical density (OD) is measured to calculate the mass (O'Toole et al. 2000; Sauer et al. 2002). The structure of biofilms can be studied using various techniques, such as scanning electron microscopy, transmission electron microscopy, atomic force microscopy, and confocal laser scanning microscopy (Smith 2005). Nevertheless, every method requires an in vitro cultivation of biofilms, which is time-consuming, costly, and labor-intensive (Zareef et al. 2020). Moreover, there is limited information on interactions between strains and compounds in biofilms. Therefore, these methods cannot be applied in clinical diagnostics. Unlike other spectroscopies, Raman spectroscopy is label-free, quick, and contact-free. In this way, biomarker spectra can

be obtained without invasive procedures. Bacteria can be identified using spectral information and statistical methods (Cui et al. 2019).

Table 1. A list of Raman studies on bacteria and biofilm

Type of Microorganism	Output
Protozoa cells	Characteristic peaks of polysaccharides (1382,1585 cm^{-1}) [51]
Heterotrophic biofilm	Polyanionic polysaccharides (1380 cm^{-1}), phenylalanine (1000 cm^{-1}) [52]
Escherichia coli *Pseudomonas putida* *Bacillus subtilis*	Microorganisms were discriminated based on the peaks of tyrosine (659 cm^{-1}), lipids (1112 cm^{-1}), proteins (1366 cm^{-1}). Identification of the changes in the spectral pattern during biofilm formation [54]
Algae and *Pseudomonas aeruginosa*	Algae biofilms contain a polysaccharide-rich matrix Bacteria biofilms contain a protein-rich matrix [60]
Escherichia coli *Staphylococcus aureus*	DNA/RNA components (678, 802, and 1570 cm^{-1}) [22]
Escherichia coli	Distinctive spectral features for monitoring bacterial death (DNA/RNA components, 678 cm^{-1}) [61]
Pseudomonas aeruginosa	Detection of pyocyanin (1088, 1125, 1352 and 1613 cm^{-1}) [64]
Pseudomonas aeruginosa	Plasmonic substrates were fabricated and used in label-free detection of pyocyanin [65]
Pseudomonas aeruginosa	C-C stretch, C-N stretch, and C-H in-plane bend modes were assigned as a marker peak of pyocyanin [66]
Brevundimonas diminuta *Staphylococcus aureus*	Discrimination peaks for the two-species model were determined Adenine (733 and 1340 cm^{-1}), guanine (665, 1340 and 1584 cm^{-1}), amide I (1704 cm^{-1}), C-H bending of proteins (1028 cm^{-1}), lipid (1460 cm^{-1}), DNA bases (1330 cm^{-1}) [68]
Pseudomonas aeruginosa *Staphylococcus epidermidis* *Candida albicans*	Identification of biofilm formation steps of the model microorganisms Detection of pyocyanin (1355 cm^{-1}) Discrimination of biofilms with using PCA [69]

In Table 1, Raman studies on bacteria and biofilm are listed. Raman spectroscopy was used in several bacterial research, as microscopic biochemical differences can be accurately characterized, discriminated, and identified at species and subspecies levels for bacteria, fungi, and yeasts (Kranjec et al. 2020). As all biologically associated molecules, such as proteins, nucleic acids, carbohydrates, and lipids, exhibit unique spectral features, Raman spectroscopy is a powerful technique for identifying different organisms (Ivleva et al. 2009; Jabłoński et al. 2013). The Raman spectrum contains several peaks corresponding to bacteria, including DNA, amino acids, carbohydrates, and lipids (Samek et al. 2014). A chemometric approach was used to identify the correlation between Raman peaks

and MRSA biofilm growth. To obtain a simple biological interpretation of the results, principal component analysis (PCA) is a powerful multivariate analysis tool for exploring and interpreting high dimensional data in many fields (Lee et al. 2021; Almeida et al. 2013; Tarhan et al. 2021; Oravec et al. 2019). The algorithm was used to determine if minor differences among MRSA biofilm stages can be differentiated based on their individual spectra. An analysis of loading plots can efficiently understand the relative contributions of each stage of biofilm formation (Samek et al. 2014; Jell et al. 2008). The optimal biofilm formation time was determined based on the Raman spectrum.

Recently, as the advantages of Raman spectroscopy in microorganisms have been highlighted, the research on direct measurement of bacteria inoculated on a solid medium is increasing. Traditionally, liquid medium bacteria samples have weak Raman signals, which require costly and complex techniques such as SERS, and poor reproducibility. Alternatively, bacterial studies on solid media can be more traceable and durable, with less sample contamination and a stronger Raman spectrum.

For the first time, Maquelin et al. demonstrated that Raman spectra can be measured directly from a solid culture medium in 2000 (Maquelin et al. 2000). Over the years, direct measurement on agar plates has been emphasized as a useful tool in studying bacteria. In 2022, Shen et al. presented a new fiber probe-based Raman technique on an agar plate to obtain more reliable and stable data for

microorganisms identification (Shen et al. 2022). These studies, however, focused only on planktonic bacteria, not biofilms. Here, the first direct observation of biofilm on a solid medium was performed. For the direct measurement, a modified agar plate was used and the Raman spectrum did not interfere with the MRSA biofilm spectrum. As a result, the biofilm growth from the inoculation stage to the departure stage was consistently and rapidly monitored. In order to confirm the formation of biofilm, the Congo Red Agar assay was performed in accordance with the experiment.

Raman spectral data collected from MRSA biofilms were used to test the antibacterial efficacy of natural products. Since MRSA biofilms are resistant to antibiotics, searching for treatment from medicinal plants is important. Eugenol, an antimicrobial compound with natural properties, could help reduce antibiotic use. Various food products and cosmetics have used eugenol (4-allyl-2-methoxyphenol). In another research, eugenol is proven to be antimicrobial, antioxidant, anti-inflammatory, anticarminative, and antispasmodic (Gill et al. 2004; Hashimoto et al. 1988; Mohammed et al. 2009; Moon et al. 2011; Yadav et al. 2015). Herein, eugenol exhibits antimicrobial activity against MRSA biofilms. The effect of eugenol on MRSA biofilms at different timelines was analyzed by Raman spectroscopy. The efficacy of eugenol was tested on different biofilm phases, and the most potent time to apply antibiotics to the biofilms was similar to that based on colony forming units (CFUs) on anti-biofilm tests.

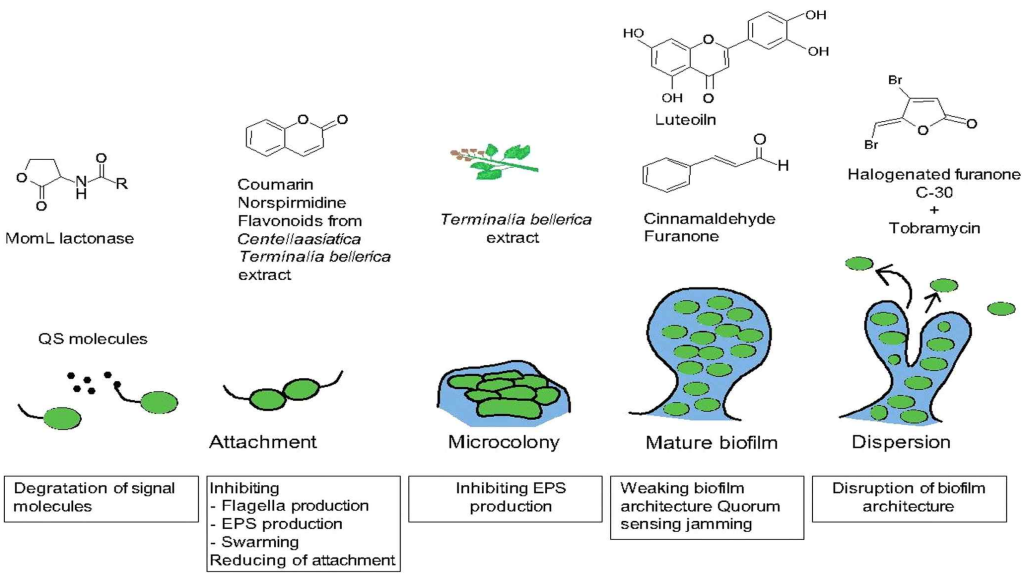

Figure 3. Natural biofilm agents in different stages of biofilm (Paluch et al. 2020)

Figure 3 represents natural biofilm agents are applied at different phases of biofilm life cycle (Paluch et al. 2020). Biofilms are known to require up to 1000 times stronger antibiotics than planktonic cells. In particular, MRSA is resistant to antibiotics, so it is essential to find a suitable antibiofilm agent. In figure it was found that the antimicrobial performs differently depending on the growth stages of the biofilm. Among them, many substances were derived from natural products, and in this study, we tried to find antibiofilm agents effective in removing MRSA from natural substances.

Previously reported natural products that perform antibacterial activities are shown in **Table 2**.

Table 2. The anti bacterial agents from natural products

Compound	Biological Source	Biological action	Reference
Thymol (terpenoid)	Origanum (spice) and thyme (*Thymus sp.*) extracts	Antibacterial activity against Streptococcus mutans. Antibiofilm activity and inactivating mature biofilms of Listeria monocytogenes	Botelho et al. (2007) Upadhyay et al. (2013)
Carvacrol (thymol isomere) (terpenoid)	Origanum (spice) and thyme (*Thymus sp.*) extracts	Antibacterial activity against Antibiofilm activity and inactivating mature biofilms of L. monocytogenes	Ultee et al. (1999) Botelho et al. (2007) Upadhyay et al. (2013)
Eugenol (phenol)	Cinnamon and clove (*Syzygium aromaticum* and *Eugenia caryophillis*) extracts	Antimicrobial action against Helicobacter S. aureus, S. epidermidis, Streptococcus pneumoniae, S. pyogenes, Salmonella typhimurium DT104 and E. coli O157:H7 Antibiofilm activity and inactivating mature biofilms of L. monocytogene	Ali et al. (2005)Kamatou et al. (2012) Upadhyay et al. (2013)
(+)-Catechin hydrate (flavonoid)	Tea (*Camellia sinensis*) and Vitis rotundifolia extracts	Antibacterial activity against Vibrio cholerae O1, S. mutans and Shigella Antibiofilm activity against Eikenella corrodens	Toda et al. (1991) Shimamura et al.(2007) Matsunaga et al. (2010)
Genistein (flavonoid)	Soybean (*Glycine max*) extracts	Antibacterial activity against S. aureus, B. anthracis and Vibrio fluvialis	Hong et al. (2006)
Gallic acid Phenolic acid	*Vitis rotundifolia* extracts	Antimicrobial activity against P. aeruginosa ATCC 9027. Antibiofilm activity against E. coli, P. aeruginosa, L. monocytogenes and S. aureus.	Rauha et al. (2000) Borges et al. (2012)
Protocatechuic acid	*Scrophularia frutescens*	Bacteriostatic effect against Micrococcus luteus	Fernández et al. (1996)

(phenolic acid)	extracts	YMBL and P. aeruginosa ATCC 9027 Antimicrobial activity against L.monocytogenes	Rauha et al. (2000)
Hydroquinone (phenol)	Bilberry (*Vaccinium myrtillus*)	Slightly inhibited the growth of Mycobacterium leprae Alters the agglutination of S. mutans induced by sucrose	Drea (1944) Himejima et al. (2004
Cranberry (polyphenols)	American cranberry (*Vaccinium macrocarpon*) marketed as Urell	Inhibition of E. coli adherence to mucosal surfaces. Inhibited both the growth and biofilm production by Staphylococcus spp.	Schmidt and Sobota (1987) LaPlante et al. (2012)
p-Hydroxybenzoic acid (monohydroxibenzoic acid)	*Scrophularia frutescens* and *Scrophularia sambucifolia* extracts	Antimicrobial effect against of Ganoderma boninense	Fernández et al. (1996) Chong et al. (2009)
Resveratrol (stilbenoid)	*Vitis vinifera* extract	Antimicrobial effect against B. cereus ATCC 11778, S. aureus ATCC 25923 and Enterococcus faecalis ATCC 29212. Antibiofilm action against P. acnes, and E. coli O157:H	Paulo et al. (2010) Coenye et al. (2012) Lee et al. (2013)

This study provides a better understanding that a particular natural anti-biofilm molecule exhibits a different mode of actions and biofilm inhibitory activity against more than one pathogenic species. Especially, effects of terpenoids, flavonoids, and phenol-based substances were studied against Staph strains, *E.coli*, and *Pseudomonas aeruginosa*.

In this study, in situ Raman monitoring was developed to observe the growth of biofilms on solid medium. This study aimed to build a tool to directly monitor biofilms at different stages, which allows the subsequent identification of the optimal time to eradicate growing biofilms. We have developed a new technique for nondestructive monitoring of the growth of drug-resistant biofilms and to detect the optimum condition for effective antimicrobial activity. Therefore, the tool offers a simple, rapid, and inexpensive analysis of life threatening clinical infections.

1.2. Purpose of research

Raman analysis was performed in situ on biofilms of methicillin-resistant Staphylococcus aureus. Analytical conditions and experimental environment for direct analysis of resistant microorganisms were established. Biofilm stages were classified using multivariate analysis methods such as PCA, PLS-DA, and PLSR. The antibiofilm dosing time of the eugenol was predicted. In this study, we presented that Raman can be applied as a sensitive, in situ fingerprinting tool to study unknown natural product antibiotic ability. In this way, the Raman spectra of bacteria can be obtained within several seconds, making it a rapid detection tool.

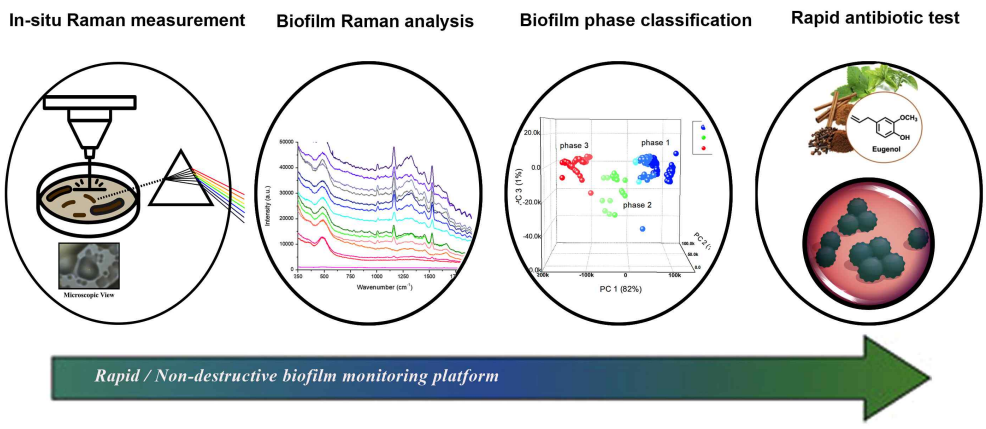

Scheme 1. Non-destructive biofilm monitoring platform

Chapter 2. Experimental Section

2.1. Materials

2.1.1. Chemicals

Eugenol was purchased through Tokyo Chemical Industry (Tokyo, Japan). Vancomycin hydrochloride was purchased through Sigma Aldrich (Seoul, Korea). Congo red dye (Daejung chemicals, Siheung-si, Korea) and saccharose (Sigma Aldrich; Seoul, Korea)

2.1.2. Microorganisms

MRSA USA 300 was obtained from Professor Chung (Chung don won) Dongduk women's university. E. coli and Staph epidermidis was obtained from Korean Collection for type Cultures.

2.1.3. Bioassay reagents

- Phosphate-buffered saline (PBS) and dimethyl sulfoxide (DMSO) (Thermo Fisher sci., Waltham, MA, USA)

- Tryptic soy broth (TSB), tryptic soy agar (TSA), and brain heart

infusion agar (BHI); (Difco, Becton Dickinson, and Company, Franklin lakes, USA)

- 3M Petrifilm staph express count plate, plastic spreader, and phosphate-buffered dilution water (3M, St. Paul, MN, USA)

- Crystal violet solution (Sigma Aldrich, St. Louis, MO, USA)

2.1.4. Experimental instruments

Clean bench: Class II Biological Safety Cabinet,

ESCO®- CO2 incubator: Forma Series II water jacketed CO2 incubator, THERMO

FTIR (Bruker, Billerica, MA USA)

Microscope (Nikon, Japan)

Raman spectroscopy (Nanophoton Co., Osaka, Japan)

Fluorescence microplate reader: Spectra Max Gemini XPS, Molecular Devices,(San Jose, CA, USA)

2.2. Methods

MRSA USA 300 was obtained from Professor Chung (Chung don won) Dongduk Women's University in this study. All aqueous solutions were prepared using ultrapure water. Phosphate-buffered saline (PBS) and dimethyl sulfoxide were purchased from Thermo Fisher Scientific (Waltham, MA, USA). Tryptic soy broth (TSB; Difco, Becton Dickinson, and Company, Franklin Lakes, NJ, USA), tryptic soy agar (TSA; Difco, Becton Dickinson, and Company, USA), and brain heart infusion agar (BHIA; Difco, Becton Dickinson, and Company, USA) were used to culture bacteria. Congo red dye (Daejung chemicals, Siheung-si, Korea) and saccharose (Sigma Aldrich; Seoul, Korea) were used for a Congo red assay (CRA). Then, a 3M Petrifilm staph express count plate (3M, St. Paul, MN, USA), plastic spreader, and phosphate-buffered dilution water were all purchased from 3M to calculate CFUs per mL. The reagents and media were sterilized in an autoclave at 121 °C for 15 min before use. Vancomycin hydrochloride was purchased through Sigma Aldrich (Seoul, Korea). The antibiotic powders were dissolved in double-distilled water to produce antibiotic stock solutions (10 mg/mL). Eugenol was purchased through Tokyo Chemical Industry (Tokyo, Japan).

2.2.1. Preparation of agar plates

It is necessary to differentiate staphylococci based on their biofilm phenotypes to clarify their impact on infection diagnosis (Raad et al. 1995). The phenotypic characterization of MRSA was performed on a Congo red agar with 0.8 g of Congo red dye and 36 g of saccharose on 1.0 L of BHI agar (Freeman et al. 1989). First, an MRSA strain was grown in TSB at 36°C for 24 h for activation. Then, 200 µL of sub-cultured microorganisms (OD600 = 1) was streaked on CRA and incubated at 37°C for 24 h. Red color of the former colonies indicated negative results, whereas black indicated positive results (Jebril 2020).

In addition, a new agar plate was developed to serve as a substrate for growing biofilms to be analyzed with Raman spectroscopy. A modified BHI agar (MBHIA) was established for Raman spectroscopy sample preparation. Initially, the biofilm on CRA plates was measured directly; however, the fluorescence peaks from the staining obscured the peak, making accurate measurements impossible. Hence, various agar plates were compared to develop a Raman-optimized biofilm medium. In the study by Freeman et al., 5% sucrose supplementation in the BHI broth is used to induce biofilm on an agar plate (Freeman et al. 1989). Therefore, the modified BHI agar plate included BHI broth and 5% sucrose without the Congo red dye. Then, 200 µL of activated MRSA was streaked on MBHIA and incubated at 37°C. Biofilm formation on MBHIA was directly monitored from the agar plate by Raman spectroscopy from 0 to 48 h

(Jebril et al. 2020). For the direct measurement, a modified agar plate was used and the Raman spectrum did not interfere with the MRSA biofilm spectrum. As a result, the biofilm growth from the inoculation to the departure stage was consistently and rapidly monitored. To confirm the biofilm formation, the Congo red agar assay was performed based on the experiment.

Table 3. Different solid culture mediums ingredients

Composition/Liter	Congo red agar	Modified BHI agar	Tryptic Soy agar
Congo red dye	0.8 g	…	…
Sucrose	36 g	36 g	…
Water	1 L	1 L	1 L
BHIA	52 g	52 g	…
TSA	…	…	40 g

2.2.2. Direct measurement of biofilm growth on solid culture medium

A fast and reliable detection and identification of microorganisms is crucial in environmental science, for food quality as well as medical diagnosis. Bacteria are therefore required to be cultured only until biofilm are formed; biofilm here are defined as colonies that develop in 5 h of growth after plating and have average colony diameters of 10−110 μm (depending on the type of microorganism). Raman spectra can be directly acquired from the biofilm on solid culture media. When performing measurements on microorganisms still growing on the solid culture medium, there are minimal sample preparation steps prior to spectral acquisition. Since spectra with good signal-to-noise ratios can be obtained of biofilm within a few minutes of signal collection time, this Raman spectroscopic approach offers the potential for rapid identification of microorganisms. However, a major obstacle of this approach is the presence of signal contributions from the underlying culture medium in the bacteria Raman spectrum due to the limited thickness of the biofilm. Because the medium signal contribution is neither negligible nor constant, it will interfere with strain identification. We have developed a new approach to deal with this problem. The newly created MBHI agar plate signal does not interfere with biofilm spectra. As a result, the cultured microorganism on solid culture medium was directly measured by Raman spectroscopy to monitor the formation of biofilm.

(a)

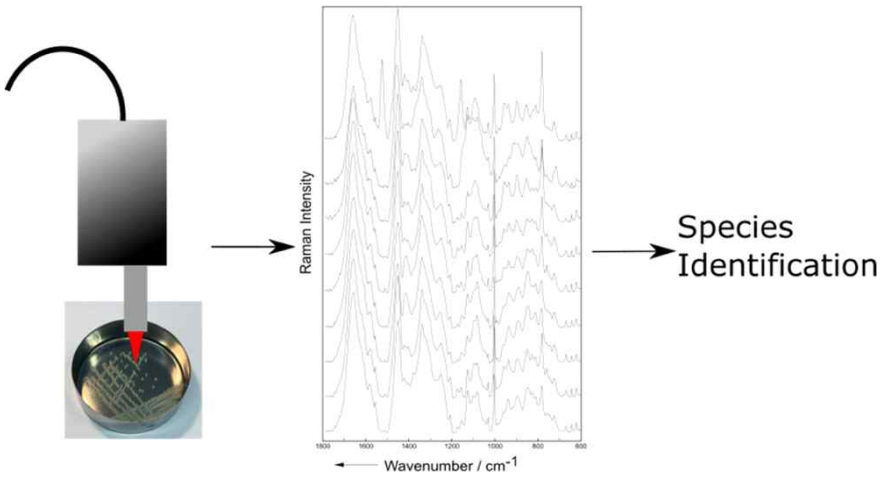

(b)

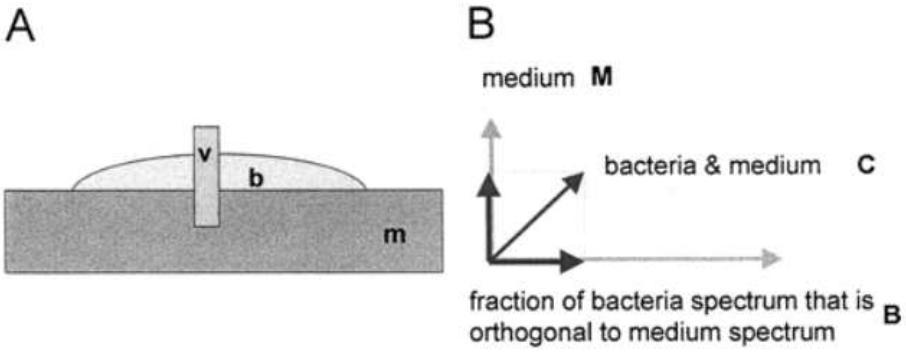

Figure 4.(a) Fiber Probe-Based Raman Spectroscopic Identification of Pathogenic Infection Microorganisms on Agar Plates (shen et al. 2022) (b) Diagrammatic representation of the measurement volume during sampling of a bacterial microcolony on a solid culture medium (m). (Maquelin et al. 2000)

2.2.3. Preparation of microorganism sample

MRSA strains were individually grown in TSB at 37°C for 24 h for activation. Then, 200 µL of sub-cultured microorganisms (OD 600 = 1) was inoculated on MBHIA. In order to monitor biofilm formation by Raman spectroscopy, the microorganisms were incubated on agar surfaces 0 - 48 h after inoculation. The incubation time refers to the duration the microorganisms were incubated on agar plates prior to Raman measurements. Bacterial isolates were grown overnight on agar plates, using the media and incubation conditions and adjusted to an optical density (OD) of 0.15 before incubation. To test if the bacterial density (CFU/mL) affected the Raman spectra, samples were cultured after 24 h and adjusted to OD 0.1, 0.3, and 1.0. To calculate the CFU/mL, a five-fold serial dilution was performed in PBS at each OD, and colonies were counted at a dilution that gave between 10 and 30 colonies per 10 µL. To test if the phase of growth affected the Raman spectra, samples were cultured after 24 h and the samples were adjusted to an OD of 0.3, to ensure a consistent bacterial density between samples. After incubation, 1 mL was centrifuged at 9000 rcf for 3 min, the bacterial pellet was washed 3 times with PBS, and the supernatant was discarded. Dried drops were sonicated for 5 min. Each isolation was reproduced three times.

2.2.4. Anti-biofilm assay

To measure the efficacy of antibiotics against MRSA, minimum inhibitory concentrations (MICs) were determined. MIC is the lowest concentration of antibiotics that inhibits the visible growth of microbes overnight (Taofiq et al. 2019). The MICs of vancomycin and eugenol for MRSA were detected using the microdilution method. The minimum biofilm inhibition concentration (MBIC) is the lowest concentration of antibacterial agents that yields no colonies compared to the initial inoculum (Uppu et al. 2017).

Eugenol was evaluated in an anti-biofilm assay. MRSA biofilms pre-formed over 24 h were treated in a conical tube with 416 μg/mL (MIC) and 1024 μg/mL (2×MIC) of eugenol. Biofilms prepared without eugenol were used as controls. To determine the CFU/mL of the biofilms, the biofilms were washed and counted (Uppu et al. 2017). All determinations were done in triplicates.

The effect of eugenol on biofilms was tested after 5 h and 36 h by rinsing the biofilms in PBS to remove planktonic bacteria and exposing them to varying eugenol concentrations at 37°C. Then, the biofilms were again washed with PBS, sonicated, and dissolved in 200 μL of PBS. These diluted samples were plated and grown on MBHI agar and viable CFUs per mL were determined. The Petrifilm was used to check the biomass of the biofilms at different stages. Tests were conducted in triplicates, and the result was expressed as

activity in terms of μg of extract per mL. In parallel to Raman experiments, antibiotics on cell viability were tested in liquid broths with the same inoculum and reagents. The experiments were triplicated on different dates.

2.2.5. Quantification of biofilm cell counts on petrifilm

Petrifilm count plates were used to evaluate the antibacterial effect of different concentrations of eugenol and vancomycin against MRSA. Antibiotic samples were ultrasonicated for 15 min before use. Each sample had an initial concentration of 1.0 OD 600 nm prepared in a TSB medium. The MIC and MBC of eugenol and vancomycin were added to the medium and incubated at 37°C for 4 h at 180 rpm. After incubation, Petrifilms were used to enumerate the efficacy of antibiotics (CLSI 2018). The samples were diluted 10 times, and 1 mL was inoculated on a 3M Petrifilm count plate and modified TSA and incubated at 37°C for 24 h.

According to 3M Petrifilm interpretation guidelines, bacterial colonies were counted after incubation. Red-violet colonies were counted as the total bacteria (Silbernagel et al. 2003). The inoculated sample on agar plates was analyzed by Raman spectroscopy to evaluate the antibacterial effect of antibiotics.

2.2.6. Raman instrumentation

The experiments were conducted using Raman spectroscopy (RAMANtouch, Nanophoton Co., Osaka, Japan) with a single-mode diode laser at 785 nm. An objective microscope lens (Nikon, Japan, 50x, numerical aperture 0.5, working distance 500 μm) was used for focusing the laser beam. The laser spot dimension was approximately 0.6 μm × 1.0 μm. Raman-dispersed light was collected through the same objective lens, passed through a 50-μm pinhole slit, and scattered via holographic grating (300 lines/mm) onto a thermoelectrically cooled (−70°C), deep-depleted, charge-coupled device (1340 × 400 pixels, Teledyne Princeton Instrument, Trenton, NJ, USA). Before and after experimental measurements, an internal silicon standard at 520 cm^{-1} was used to confirm system alignment and light throughput to the sample. A laser power of 30 mW and exposure time of 50 s were used for all Raman experiments.

2.2.7. Analytical condition

In order to set up the experimental condition, the optimal laser power, lense, and exposure time was set through sample analysis. The full fingerprints of biofilm was analyzed from 100 to 2000 cm^{-1} wavelength. In general sample analysis, 532 laser of Raman is used and the 785 laser is mainly used for biosamples that may have high fluorescence or weak signals. Also in this research the 785 laser was used to obtain biofilm spectra.

Table 4. Test anlytical condition to obtain the best fit biofilm raman spectra

Sample region	Time	Laser type (nm)	obj. lens	Laser power (mw)	exposure time (sec)	ave. (time)
top of biofilm	2:07	532	20X	3.80	10	5
	2:10	532	20X	2.54	20	10
	2:29	532	20X	22.9	1	10
	2:32	532	20X	4.30	10	10
	2:36	532	20X	4.72	10	1
	2:41	785	20X	27.2	1	1
	2:41	785	20X	27.3	20	5
	2:49	785	20X	27.5	30	5
	3:26	785	20X	22.2	30	10
	3:35	785	20X	22.3	40	1
	4:11	785	20X	11.6	10	1
	4:18	785	20X	21.3	40	1
	4:22	785	20X	21.3	40	1
	4:24	785	20X	21.3	20	1
	4:31	785	20X	21.3	30	5
	4:36	785	20X	21.4	30	5

	4:39	785	20X	21.4	30	5
	2:15	785	20X	20.1	30	5
	2:24	785	50X	20.1	30	5
	2:27	785	50X	20.1	40	10
	2:34	785	50X	20.2	40	7
	2:39	785	50X	20.2	40	5
	2:46	785	50X	20.2	30	5
	2:52	785	50X	20.2	30	5
	2:57	785	50X	20.3	30	10
border	3:07	785	50X	20.3	30	3
	3:11	785	50X	20.3	40	5

Table 5. Optimized analytical condition for MRSA biofilm growth

Measurement Condition	
Excitation Wavelength	785 nm
Excitation Power	30 mW
Grating	300 gr/mm
Pinhole size	50 μm
Exposure Time	50 s
Averaging	3

2.2.8. Analyses and characterizations

Analysis of variance (ANOVA) was performed to determine the antimicrobial efficacies of different concentrations of vancomycin and eugenol in the solutions. All data are presented as means of three replications. Procedures described by Association of Official Agricultural Chemists were used to calculate CFU/mL, which was converted to logarithms for statistical analysis (Silbernagel et al. 2003).

The acquired Raman spectra were baseline-corrected using multiple scatter correction before performing the multivariate analysis of PCA using commercial unscrambler software (Aspentech, Bedford, USA). The PCA scores of the first and second principal components were used to plot 3D charts, based on which the degree of similarity and difference of Raman spectra of biofilm grown at different times was analyzed.

PCA algorithms were used to develop models that allow discrimination and classification of biofilm growth stages using the spectral characteristics of MRSA biofilms. SIMCA-P 17.0 (Umetrics, Umeå, Sweden) software was used to conduct PCA and PLS-DA data analysis. Graphs were reated using Origin 8.0 (OriginLab Corp., Northampton, MA, USA).

2.2.9. Data Preprocessing

Data preprocessing was conducted using Unscrambler software 10.1(Aspentech, Bedford, NJ, USA) to baseline correct before the construction of chemometric models. The baseline correction helped to remove the background fluorescence from MRSA biofilm cells. In order to perform chemometrics, the Savitzky–Golay algorithm was performed to smooth the Raman spectra. Additionally, the standard normal variate (SNV) method was conducted to normalize the spectra.

Chapter 3. Results and Discussion

3.1. Developing natural products as potential antibiofilm agents

Biofilm-linked infections are not easy to treat due to multidrug-resistant microbes. Low efficiency of various treatments and *invivo* toxicity of available antibiotics drive the researchers toward the discovery of many effective natural anti-biofilm agents. Natural extracts and natural product-based anti-biofilm agents are more efficient than the chemically synthesized counterparts with lesse sideeffects. These natural compounds have different impacts depending on biofilm stages, so it is important to predict the optimal administration time. The antibiofilm test was analyzed by Raman to rapidly test the antibacterial activity of novel natural biofilm substances. The tested results were cross validated with the calculation of CFU/mL to confirm the effectiveness.

3.1.1. Disk diffusion assay: Antibiotic effects of natural compounds

Disk diffusion assay was carried out to test the susceptibility of natural substances found in the previous literature. the assay is used to screen biological material and drug candidates for antibacterial activity. It is a qualitative assay that commonly performed to evaluate the antimicrobial activity of phytochemicals or extracts. The density of MRSA bacteria was standardaized to 1 X 10^{8} coliform units (CFU/mL). An effective antibiotic will produce a circular zone of inhibition around the disk and the size is measured. As a result of the assay, other substances did not show suceptibility to MRSA, but the eugenol showed an antimicrobial effect by forming a inhibition zone.

Table 6. List of compounds tested for disk diffusion assay

	Compound
1	Control(DMSO)
2	Eugenol
3	Baicalin std.
4	Scutellaria Baicalensis Root Extract
5	Quinic acid
6	Ginsenoid
7	Acetominophen
8	Betaine
9	Loganin'
10	O-coumaric acid
11	Berberine

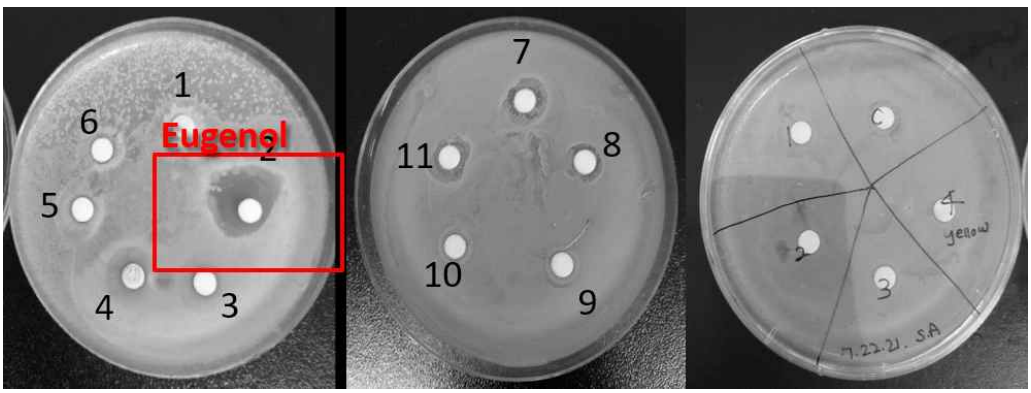

Figure 5. Disk diffusion assay result after application of natural compounds

3.1.2. Eugenol as potential antibiofilm agenet

Eugenol is a colorless to pale yellow, aromatic oily liquid extracted from essential oils especially from clove, nutmeg, cinnamon, basil and bay leaf. It is used as a flavor or aroma ingredient in teas, flavorings, and essential oils. It is also used as a local antiseptic and anaesthetic. Eugenol, an antimicrobial compound with natural properties, could help reduce antibiotic use. Various food products and cosmetics have used eugenol (4-allyl-2-methoxyphenol). In another research, eugenol is proven to be antimicrobial, antioxidant, anti-inflammatory, anticarminative, and antispasmodic (Gill et al. 2004; Hashimoto et al. 1988; Mohammed et al. 2009; Moon et al. 2011; Yadav et al. 2015). Herein, eugenol exhibits antimicrobial activity against MRSA biofilms.

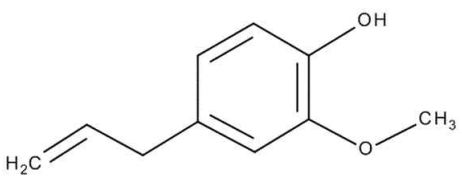

Figure 6. Structure of Eugenol

3.1.3. Determination of MICs and MBICs to test the effectiveness of antimicrobials against MRSA

MIC is the minimum concentration of an antimicrobial that prevents bacteria from growing after overnight incubation for MRSA strain (Taofiq et al. 2019). Also, the MBIC is the minimum biofilm inhibitory concentration (Ceri et al. 2001). Microdilution was used to detect the MICs and MBICs of vancomycin and eugenol. In this study, the control was untreated biofilms to represent the growth of bacterial cells. The MIC and twice the MIC of vancomycin were used as negative controls. It is the most known lethal antibiotic treatment for MRSA. Natural compound, such as eugenol, was selected as a possible traditional antibiotic that could inhibit the growth of planktonic and biofilm MRSA. The values of MIC and MBIC of eugenol were measured to test the effectiveness of the optimal antibiotics for the microorganism. As a result, the MIC of vancomycin for MRSA was 2 μg/mL. For MRSA, eugenol had MIC values of 416 - 1024 μg/mL, and its MBIC values were twice the MIC (Yadav et al. 2015; Moses et al. 2020).

3.2. Detection of the biofilm formation phenotype

When planktonic bacteria come into contact with a solid surface such as the inner surface of a water pipe, biofilms start to develop. Depending on the genus and species, attached bacterial cells start to produce a diverse range of macromolecules (Abbanat et al. 2014), so-called extracellular polymeric substances (EPS) suchas lipids, nucleic acids, proteins, and polysaccharides. The final biofilm consists of the cells of a large variety of microorganisms encased in a complex matrix of macromolecules in which the cells are embedded and protected (Stöckel et al. 2016). Several methods have been developed to identify biofilm from planktonic bacteria. In this study, these methods have been compared to select the best method to analysis biofilm formation.

3.2.1. Congo Red Agar assay(CRA)

The CRA developed by Freeman et al. is the standard method for observing biofilm formation. The biofilm phenotype is tested on Congo red agar, which identifies biofilm bacteria as black colonies and nonbiofilm bacteria as pink or red colonies [32]. MRSA was grown on Congo red agar plate to confirm the biofilm formation. In

Figure 7, MRSA produced black colonies after 24 h of incubation. To observe the physical development of biofilms, the sample was carried out on Congo red agar. MRSA inoculated for 1 h showed red pigmentation, but it developed biofilm on CRA agar after 24 h of incubation, and a black pigmentation was observed. After 48 h of incubation, the biofilm formed a strong black cluster all over the agar (Figure 7). However, it was difficult to determine when a colony of bacteria attaches to form biofilms. In most studies, CRA could not differentiate between strong, moderate, and weak biofilm producers (Panda et al. 2016). Since colonies of bacteria growing on agar plates were surface-adhering biofilms (Abbanat et al. 2014), a new modified MBHI plate was used to observe the growth of biofilms. Raman spectroscopy was used to monitor the chemical changes MRSA goes through as a biofilm.

(a) 1 h incubation (b) 24 h incubation (c) 48 h incubation

Figure 7.(a-c) Phenotypic characterization of biofilm formation of MRSA strains on Congo red agar after 1 h, 24 h, and 48 h of incubation

3.2.2. Traditional methods of biofilm identification

Traditionally, biofilms are identified by applying crystal violet dye, and their optical density (OD) is measured to calculate the mass (O'Toole et al. 2000; Sauer et al. 2002). The structure of biofilms can be studied using various techniques, such as scanning electron microscopy and confocal laser scanning microscopy (Smith et al. 2005). However, every method requires an in vitro cultivation of biofilms, which is time-consuming, costly, and labor-intensive (Zareef et al. 2020). Moreover, there is limited information on interactions between strains and compounds in biofilms. Therefore, these methods cannot be applied in clinical diagnostics. In addition to the CRA method, the biofilm positivity was double checked by the microtiterplate and tube method, which are widely used in liquid cultivation. As a result, MRSA was positive in biofilm formation, but *E.coli* and *Staphy epidermidis* strains were negative. MRSA strain was selected for further biofilm research.

Figure 8. (a-c) Traditional methods to identify biofilm

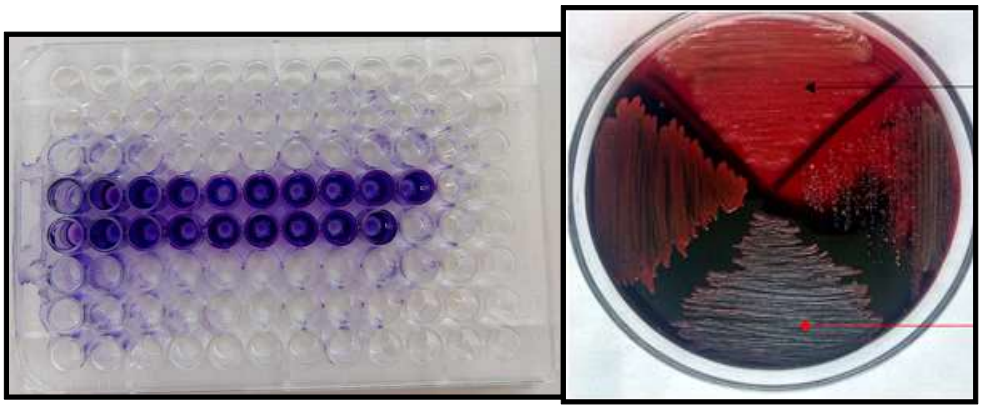

(a) Microtiterplate method (b) Congo red agar assay

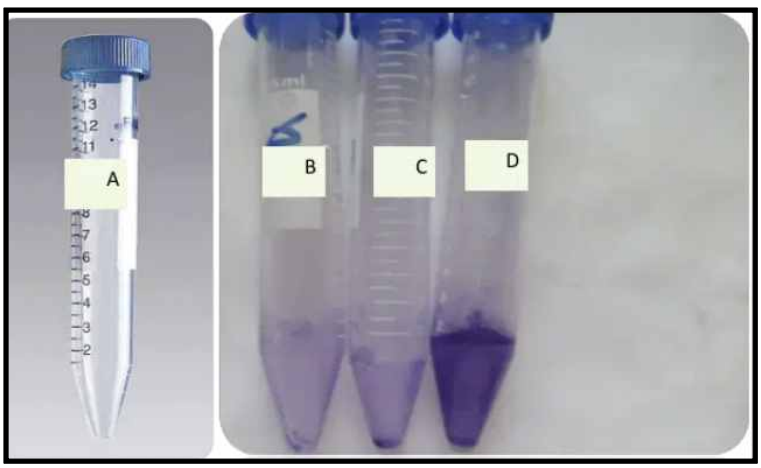

(c) Test tube method A. Negative control, B: Weak, C: Moderate, D: strong biofilm former

3.2.3. Biofilm quantification in time

In parallel to Raman analysis, the biofilm on MBHI agar was quantified hourly for 48 hours, three independent experiments were performed, each on a separate day. Colony forming unit per mL was calculated and the growth curve was presented. The growth mass of the biofilm showed three different linear fits and they were divided in different time frames. The measured growth had similar characteristics to a typical bacterial growth curve, starting with a gentle growth slope from 0h to 5 h as in the lag phase of bacterial growth, and followed by an increased slope from 5 h onwards as in the exponential growth phase. Nevertheless, the slope of the growth between 5h to 24h is smaller than the exponential growth slope of bacterial culture, which could be due to a different growth behavior of bacteria adhered to surfaces (or a biofilm) compared to planktonic bacteria, or may be possibly due to the limited nutrients available in the medium. We observed that the time window of 0 h to 5 h was a crucial time frame for biofilm attachment, since the mass accelerated during this time frame. The growth slopes can be related to the phases of biofilm. The viable bacteria from the biofilm increased more quickly on the membrane surfaces. In this way, the growth of bacteria on a surface may be evaluated more sensitively when monitoring bacterial viability during the high growth period (5 – 9h). Membrane biofilm susceptibility can therefore be judged in

significantly less time than the 24h biofilm assay and more information about the early biofilm growth can be obtained. Bacterial growth rate may vary from one day to another, and this variability is shown by the different growth curves in Figure. For this reason it is preferable to perform comparison of membranes in parallel, at the same day.

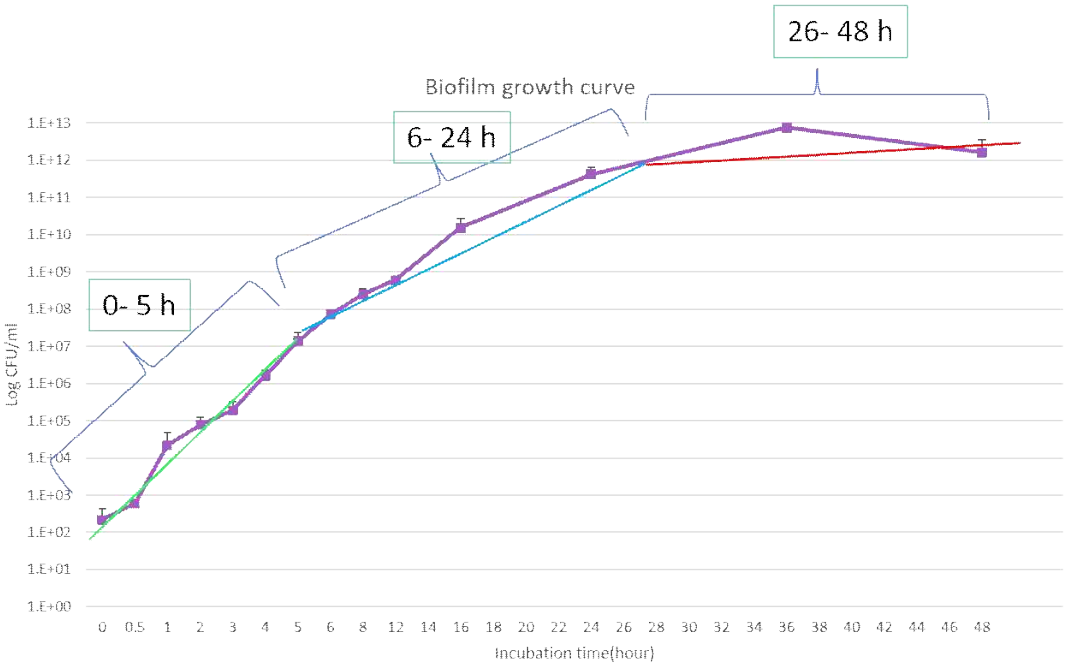

Figure 9. A curve presenting average values for biofilm quantification of the MRSA presented with linear fit (green) and a linear fit in the range of 6h to 24 h (blue), and 26 h to 48 h(red)

3.2.4. Biofilm identification by Raman spectroscopy

While these tehniques show good physical identification within a biofilm, the main limitations are the complex preparation procedure, the cost and time associated with these measurements (Ivleva et al. 2009). Optical spectroscopy techniques nowadays offer the opportunity to identify chemical compounds in high spectral resolution (Jabłoński et al. 2013), combining the power of 3D sample analysis with focused chemical composition. One of these techniques is Raman Microscopy that utilizes a laser beam with known wavelength to analyze a sample. By measuring the scattered radiation and energy shift, Raman is able to use the acquired information of a cell's chemical characteristics to differentiate species (Samek et al. 2014). This should allow for a quick, affordable and unaltered evaluation of biofilm samples with a spatial resolution of 1 µm.

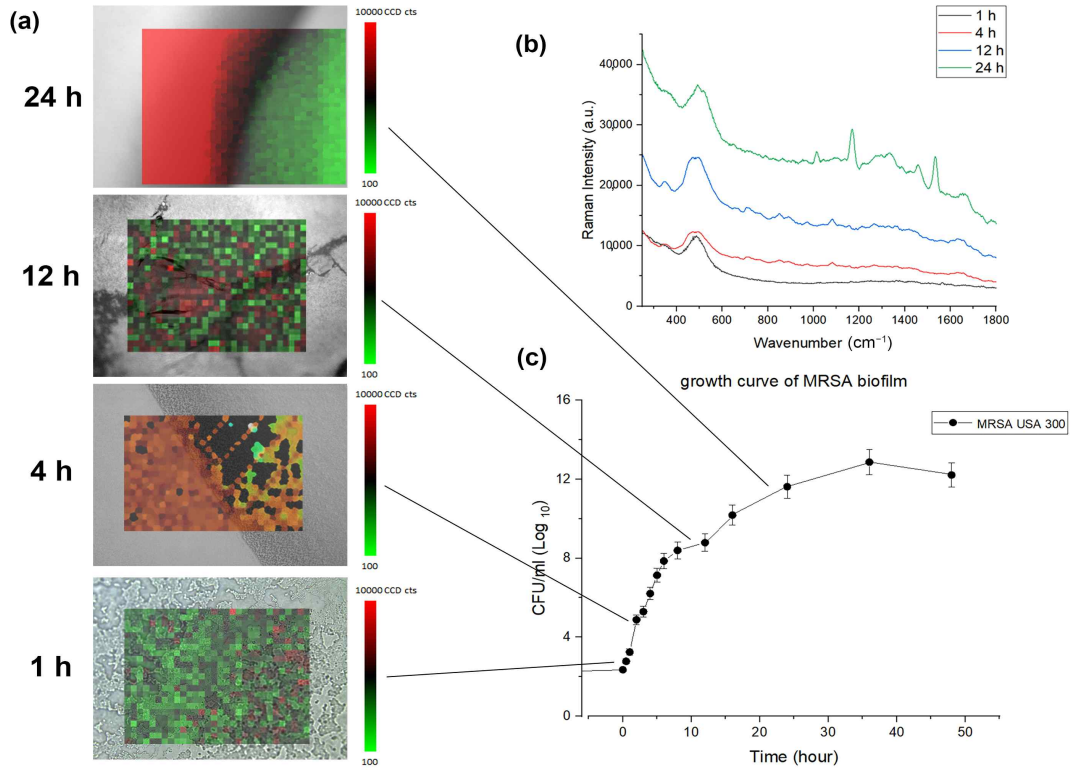

Figure 10.(**a**) Composite confocal Raman xy mapping images depicting the evolution of MRSA biofilm over time. 800 spectra (20 × 40, X × Y) were acquired across a 100 μm^2 area averaging 3 times. (**b**) average MRSA biofilm Raman spectra corresponding to each time point (**c**) growth curve of MRSA biofilm formation.

In order to differentiate the planktonic bacteria from biofilm early stage, we have performed xy mapping of biofilm by Raman spectroscopy (Figure 10). Simultaneously with Raman monitoring, biofilm development from the MBHI-sucrose agar was measured

hourly for 48 h to evaluate the early attachment of the bacteria, with three independent assessments carried out on different days. The biofilm growth curve computed the time-dependent buildup of biofilm biomass based on *xy* mapping images of the MRSA biofilm grown on a solid medium (Figure 10c). The MRSA biofilm growth curve showed a comparable growth angle to that of the typical bacterial growth curve. The slope grew slowly during the first 4 h, then exponentially from 5 to 24 h. The biofilm mass grew rapidly and displayed a high growth angle, perhaps owing to the attachment of bacteria to the surface as opposed to that of planktonic bacteria. Finally, the slope slowed down from 25 to 48 h. The three distinct growth rates in Figure 2 were closely associated with the PCA analysis. The *xy* mapping of Raman spectra was used to characterize the morphological change during biofilm growth. The Raman results showed spatial changes owing to the attachment of planktonic bacteria and the chemical alteration of biofilm at different time periods. Exemplary Raman images show a planktonic bacterial cell (1 h), initial biofilm cell attachment (4 h), biofilm colony maturation (12 h), and the conglomerate growth of biofilms on the agar surface (24 h). The morphological data and biofilm development curve show that in situ Raman spectroscopy can properly monitor biofilm progression.

3.3. Biochemical features of MRSA biofilm by spectroscopies

As an alternative to microscopy and staining methods, in 2016, a research on detection of quorum sensing of Pseudomonas aeruginosa using Raman was published in Nature Matter. In this study, both FTIR and Raman spectroscopies were compared as a analytical tool to monitor the biofilm formation ability and detect the biochemical markers. The characteristics of both spectroscopies can be examined.

3.3.1 Fourier transformed infrared (FTIR) spectroscopies

The MRSA biofilm was analyzed by FTIR, and the main peaks were assigned. The PO_2 band was at 1200 cm^{-1}, the 1300~1400 cm^{-1} correlated with Amide II, and the 1700~1800 cm^{-1} correlated with Amide I band. They were compared with references. At 2700 cm^{-1}, the CH_2 CH_3 band appeared weak, and at 3000 cm^{-1}, a very broad and large water band appeared.

One of the limitations of IR for biological sample analysis is that it absorbs the H_2O band and appear in broad peak that it overlaps with other peaks

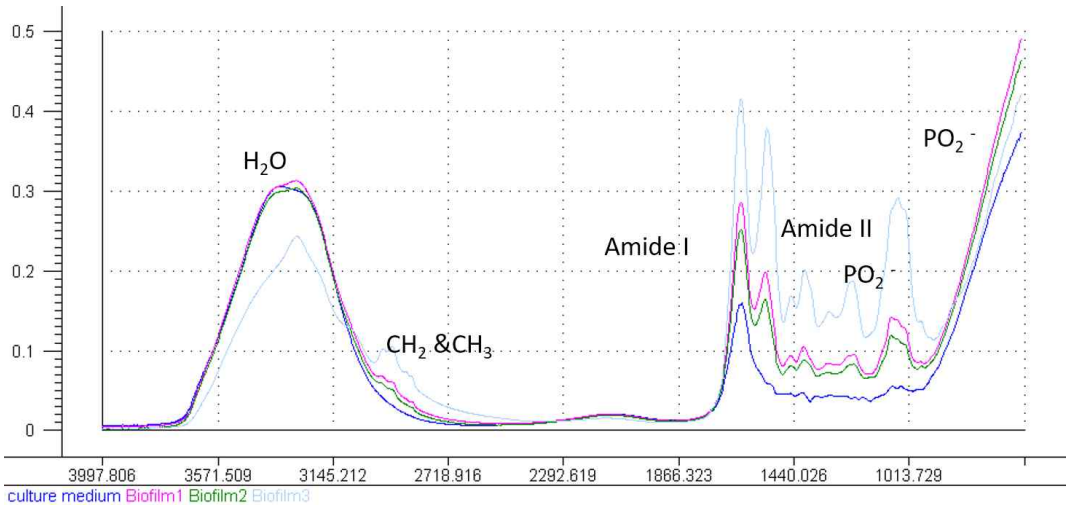

Figure 11. FTIR spectra of MRSA biofilms in a spectra range of 400 - 4000cm^{-1}

3.3.2. Raman spectroscopy of MRSA biofilm

Biofilm cells were observed under a microscope. Single cells were identified at a high magnification and conglomerate of cells attached to the surface. The cells in the conglomerate produced yellowish slime that indicated EPS. CRA was performed to confirm the formation of biofilm (Figure 7). Biofilm matrix components and their proportions are crucial to minimize and control biofilm formation. The matrix of biofilms typically consists of EPS, DNA, lipid, and extracellular vesicles (O'Toole et al. 2000; Sauer et al. 2002).

Figure 12 shows the prominent features observed in the Raman spectra of MRSA biofilms that were phenotypically confirmed. Bacterial samples were observed directly from MBHIA culture plates by Raman spectra. The Raman spectra of growth media were analyzed to identify a possible interference from the background. In Figure 12, the Raman peak at 485 cm^{-1} corresponded to monosaccharides, which are one of the ingredients for culture media, and it did not interfere with the biofilm spectra (Manilal et al. 2020).

Spectrum studies on specific chemical structures were selected from previously published studies (Table 7) (Wagner et al. 2009 35-44,46]. Fig. 1 illustrates a Raman spectrum of an average MRSA biofilm sample. The biofilm sample was at the beginning of the proliferation stage, and Raman measurement was processed in 40 mw laser power and 50-s exposure time. This was repeated 10 times.

The characteristics of biofilm samples were less sharp spectral peaks than those of single-cell bacteria. Among the key peaks in biofilm samples were DNA/RNA-related peaks at 645 cm^{-1} assigned to the COO- deformation of guanine, 785 cm^{-1} assigned to A, T (ring breathing modes in DNA/RNA bases).

Phenylalanine peak represents the existence of biofilms (Wagner et al. 2009). Peaks that are related to proteins appear as biofilms mature. The band at 1006 cm^{-1} represents the ring breathing of phenylalanine in a protein. The band at 856 cm^{-1} is attributed to the carbohydrate of C-C stretching (Xie et al. 2013). The peaks at around 1273 and 1660 cm^{-1} are mainly attributed to amide I, amide III vibrations, and carboxylic acid stretching (Sundaram et al. 2013). Most peaks were found in bacterial Raman spectra of tryptophan at 1334 cm−1, which was used for protein biosynthesis. Moreover, the CH_3CH_2 twisting mode of lipids can be found at 1450 cm^{-1} (Wickramasinghe et al. 2020).

MRSA strains can produce a golden carotenoid pigment called staphyloxanthin, which can serve as a potential antivirulence target (Xue et al. 2019). The prominent two peaks at 1158 and 1526 cm^{-1} correlate to carotenoid bands, which represent C−C stretching and C =C stretching, respectively (Ayala et al. 2018).

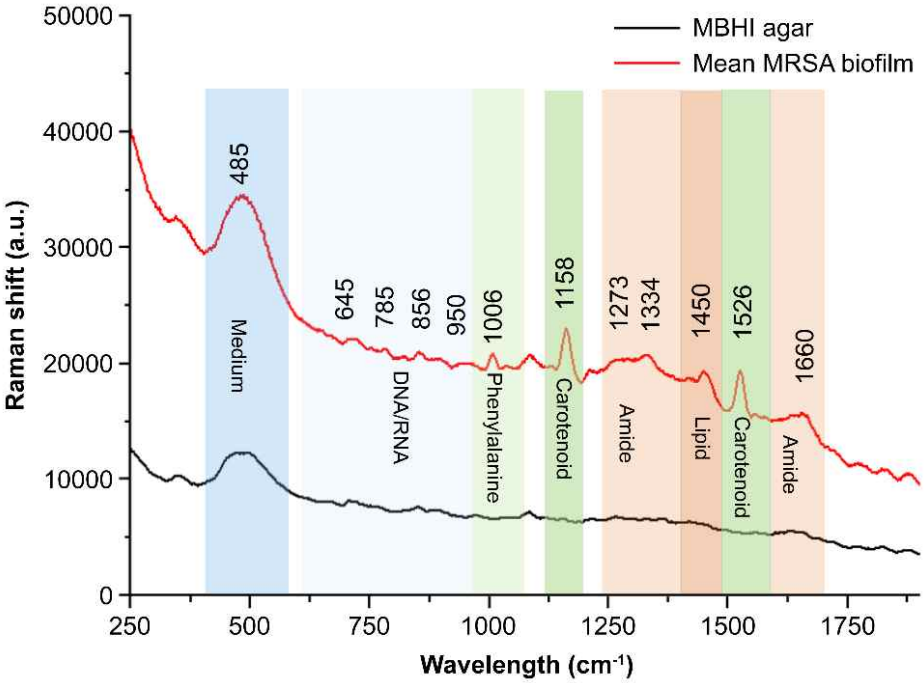

Figure 12. Raman spectra of MRSA biofilms in a spectra range of 250 - 1900cm^{-1} (regions characteristic of chemical species are highlighted).

Table 7. Raman band assignments of MRSA biofilms

NO.	Raman feature (cm^{-1})	Assignments
1	485	Monosaccharide (medium)
2	645	COO^- deformation of guanine (Chen et al. 2015)
3	785	A (adenine ring of DNA/RNA base) (Efeoglu et al. 2013)
4	856	C-C stretching from carbohydrates (Xie et al. 2013)
5	950	δ(C=C) (Xie et al. 2013)
6	1006	Phenylalanine ring breathing mode (Kao et al. 2008)
7	1158	Carotenoid (C-C) (Jarvis et al. 2004)
8	1273	Amide III of proteins (Cui et al. 2011; Wagner et al. 2009; Talari et al. 2015)
9	1334	Tryptophan (Chen et al. 2015)
10	1450	CH_2 deformation of lipids (Chen et al. 2015; Yang et al. 2011)
11	1526	Carotenoid (C=C) (Schuster et al. 2000)
12	1660	Amide I (helix) (Chen et al. 2015)

3.3.3. MRSA biofilm growth monitored for 48 h by Raman spectroscopy

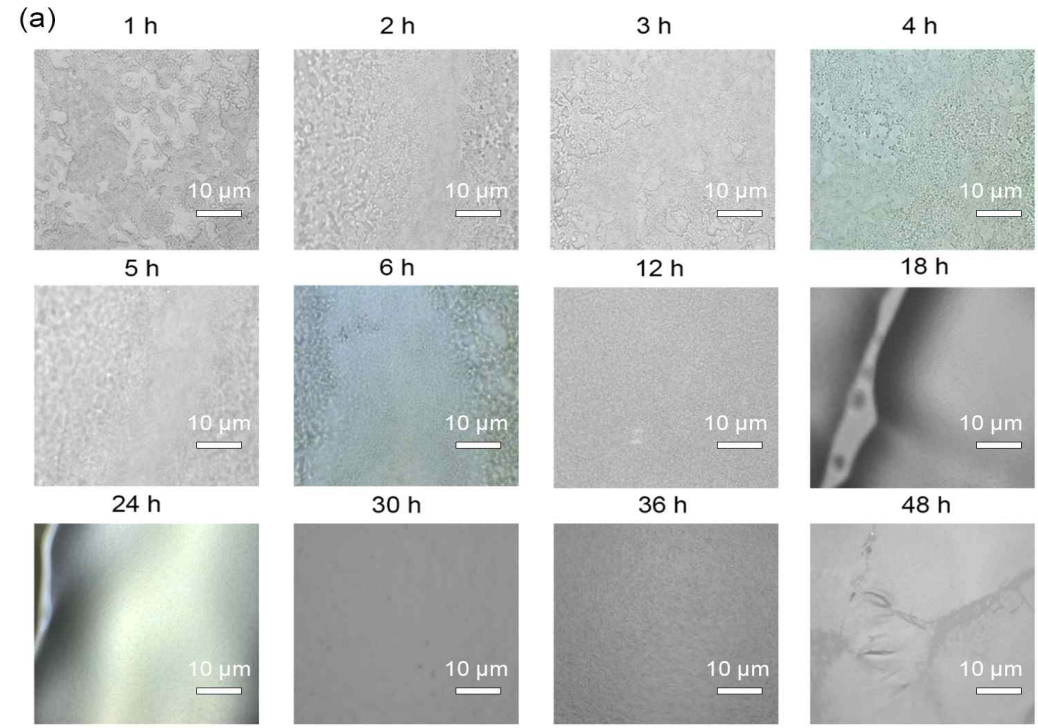

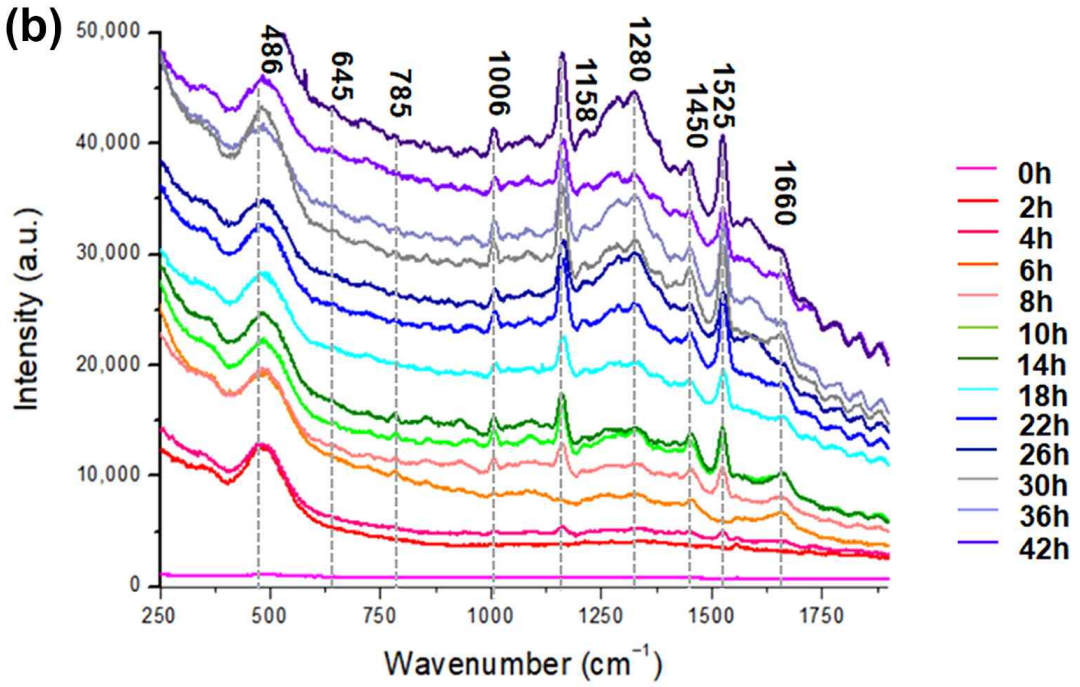

Figure 13. (a) Microscopic images of MRSA biofilms (0 - 48 h of biofilm) (b) Mean Raman spectra of MRSA biofilms every 2 h for 48h.

Raman spectroscopy was applied to chemically characterize different multispecies biofilms using specific bands identified in reference materials. Figure 13(a). shows representative microscopic images at different hours and the corresponding spectra of biofilms in Figure 13(b). Based on the signature peaks of MRSA biofilms, the growth was monitored with Raman spectroscopy from 0 h to 48 h. The dataset consists of 174 spectra of MRSA biofilms over a range of 250 cm^{-1} - 1900 cm^{-1}. Along with biofilm growth, microorganisms formed in different sizes and thicknesses. The Raman spectral data consist of different intensities and baselines due to chemical changes in biofilms over time. To correct this background spectral intensity in different stages, pre-processing was used to stabilize the baseline. The raw spectrum of biofilm growth was pre-processed using multiplicative scatter correction. Results showed that pre-processing can help in revealing the differences in the spectrum at different times.

The Raman spectrum of MRSA biofilms was acquired every 2 h for 48 h. In Figure 13(b), each spectrum was an average of 10 random points at indicated hours. At 0 h, there was no significant peak observed from MRSA biofilms. The spectra obtained at 2 h and 4 h were similar to each other, and the peak at 485 cm^{-1} from monosaccharides in the culture medium was mainly observed in the

spectrum. Starting from 4 h, very low-intensity carotenoid pigment peaks from MRSA strains started to appear at 1158 cm^{-1} and 1526 cm^{-1}.

When the incubation time increased to 6 h, a different trend of the spectrum was observed. As the incubation time increased, the carotenoid and phenylalanine peaks increased. Especially at 6 h, peaks around 700 - 800 cm^{-1} appeared in the spectrum, which represent the DNA/RNA fragments from MRSA strains. DNA/RNA-related peaks increased throughout the initial incubation period. Since the bands at 645 cm^{-1} and 1525 cm^{-1} were observed in the guanine spectrum, their intensity may reflect the changes in DNA or RNA concentrations of the biofilms (Kao et al. 2008).

From 6 h of incubation, the band at 1006 cm^{-1} from phenylalanine increased; this corresponds to lipids, proteins, and sugars (Rebrošová et al. 2019; Wang et al. 2021). It was reported the phenylalanine bands could be used as the signature peak for biofilm formation (Ebert et al. 2021). Therefore, the increase in the 1006 cm^{-1} band suggests the formation of MRSA biofilm structure. Based on these changes, it can be speculated that an early biofilm maturation begins after 6 h, and a reversible attachment phase of biofilms happened before 5 h, which is a more disruptive state of bacterial colonies.

The first significant adhesion of bacteria on biofilm surfaces was observed around 20 h, as indicated by the expression of carbohydrates and proteins. Biofilm matrix formation depends on fibrillary proteins present in the early phase of the biofilm maturation

process (Ebert et al. 2021). Early maturation, which was an irreversible attachment of planktonic microorganisms, was observed up until 24 h (Figure 13(b)). Carbohydrate bands (856 and 1158 cm^{-1}) were found to be positively correlated with the in vitro formation of biofilms. It is also interesting to note that 24-h biofilms exhibit a relative reduction in nucleic acid band intensities compared with 5-h biofilms (Ebert et al. 2021). As illustrated in Figure 13(b), the spectra from different structures of EPS matrix are characterized by strong polysaccharides (Sundaram et al. 2013) and lipopolysaccharides (Paharik et al. 2016). The initial formation of MRSA biofilms was in agreement with Congo red agar assay and microbiological analysis.

After 26 - 48 h of incubation, the overall intensity of the spectrum increased. Protein- and lipid-related bands at 1280, 1450, and 1660 cm^{-1} also increased significantly. However, the relative intensity of DNA/RNA fragment peaks decreased. The changes in the spectrum indicate that the metabolic activity of biofilms stopped, and the departure of bacteria started. Protein synthesis and lipid synthesis increase over time in response to environmental stress induced by nutrient depletion (Hoehse et al. 2012). Bacteria respond to stress by increasing their protein and lipid synthesis. During the late stationary phase, bacterial cell metabolism ceases, and thus, no DNA, protein, or lipid synthesis occurs (Moritz et al. 2010).

MRSA biofilm time points were cross-checked through viable counts (CFU/mL) and Congo red agar assay. Therefore, the monitoring of bacteria through the Raman spectrum, which is

correlated to biomarkers in biofilms, can non-destructively analyze the entire biofilm life cycle. As the biofilm life cycle progresses, the intensity of bands changes, reflecting the changes in their concentration profiles. Biofilms are structures that surround bacterial cells and serve as a shell for living systems, limiting their interaction with the environment. This process continues until the completion of biofilms, and the process was in situ analyzed with Raman spectroscopy.

MRSA biofilm formation was confirmed with Congo red agar assay and microbiological analysis. Based on Figure 13(b), MRSA biofilm formation started at around 5 h, and this was the maturation stage of the biofilms. Although it was not possible to observe any changes in the growth curve after approximately 12 h with OD and viable counts, Raman spectroscopy is sensitive enough to detect changes in bacteria from 0 h to 48 h. Unlike traditional measurements that only involved the concentration of cells in a sample, Raman spectroscopy can provide the fingerprint of DNA, RNA, protein, and lipid, which represent the physiological changes of the samples (Ren et al. 2013).

3.4. Chemometrics to analyze MRSA biofilm growth

In order to find out the classification and correlation of these abundant data, we classified the growth process of biofilm by chemometrics, that is, a multivariate analysis method. In this figure, various multivariate analysis methods are listed. It can be divided into qualitative analysis and quantitative analysis.

For algorithm calculation, the latest version 17.0 SIMCA was used as a tool to check the correlation of data. Three major multivariate analysis were performed, and principal component analysis(PCA) is performed unsupervised by reducing correlated high-dimensional data. PLS-DA is a supervised qualitative analysis method that performs categorical analysis through predictive and descriptive actual selection. PLSR is a supervised quantitative analysis that draws a calibration curve between predicted values and actual values to check the linearity of the correlation.

Scheme 2. Multivariate analysis tool

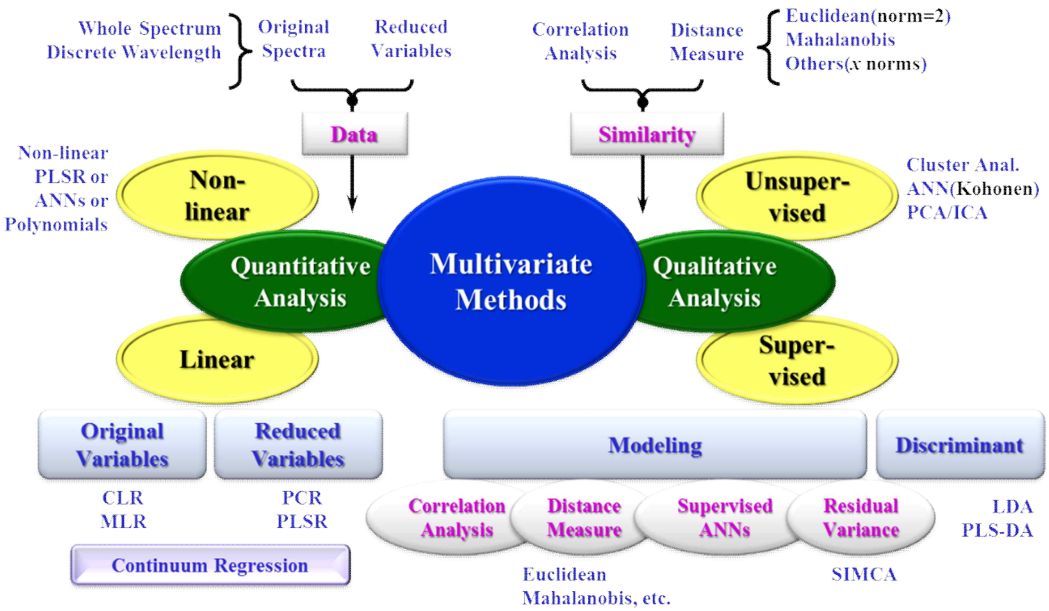

3.4.1. Data pre processing technique

First of all, the preprocessing was performed to normalize the vast amount of data. Under scatter-correction methods, we consider two preprocessing concepts: MSC and SNV. These techniques are designed to reduce the physical variability between samples due to scatter. All two also adjust for baseline shifts between samples. Multiplicative Scatter Correction(MSC) is probably the most widely used pre-processing technique for spectral data. The concept behind MSC is that artifacts or imperfections (e.g., undesirable scatter effect)will be removed from the data matrix prior to data modeling. Standard normal variate (SNV) is another frequently used pre-treatment method due to its simple algorithm and effectiveness in scattering correction. SNV is often used on spectra where baseline and path length changes cause differences between otherwise identical spectra. Between the two techniques, the most suitable method for spectral data is MSC pretreatment method.

$$x_{new} = (x_{raw} - a)/b$$

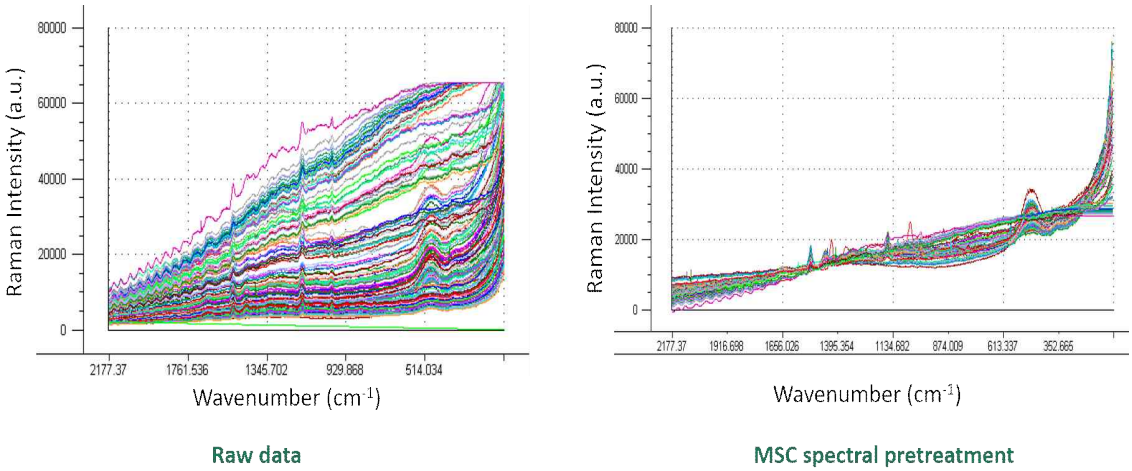

Figure 14. 171 spectral raw data after MSC pretreatment

In Figure 14 is the appearance of the spectrum after preprocessing 171 samples. You can see that the data that showed a large difference in intensity were corrected by MSC preprocessing. In spectroscopic applications, scaling differences arise from scattering effects or other general instrumental sensitivity effects. In this study, it normalized the Raman spectra intensities to identify characterize the biofilm growth.

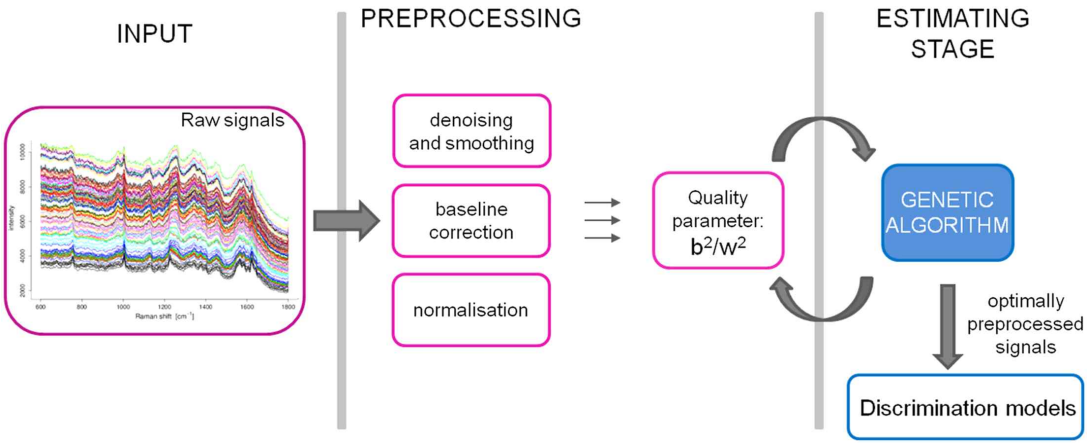

Scheme 3. Data preprocessing algorithm

3.4.2. PCA analysis to discriminate biofilm growth

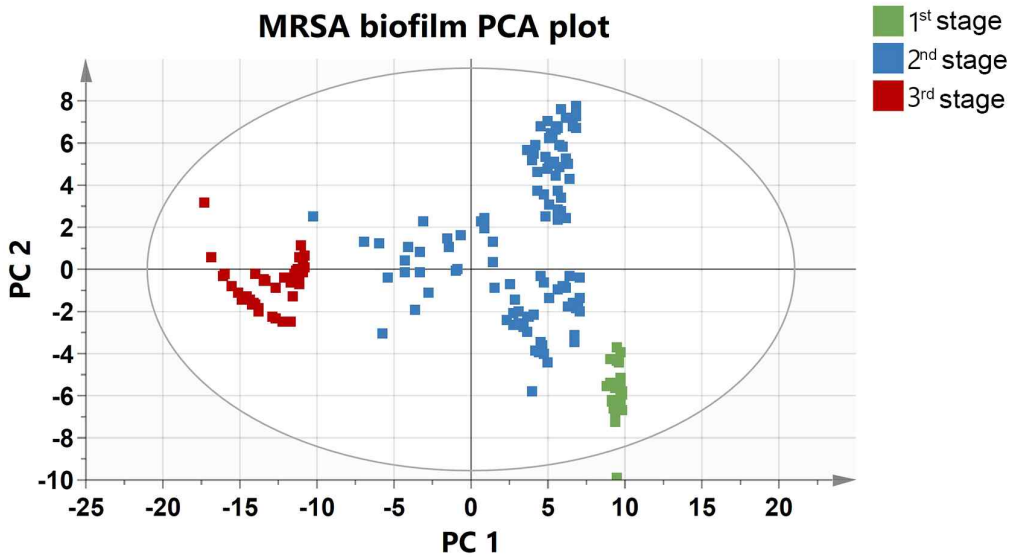

0.809, R2X[2] = 0.167, Ellipse: Hotelling's T2 (95%)

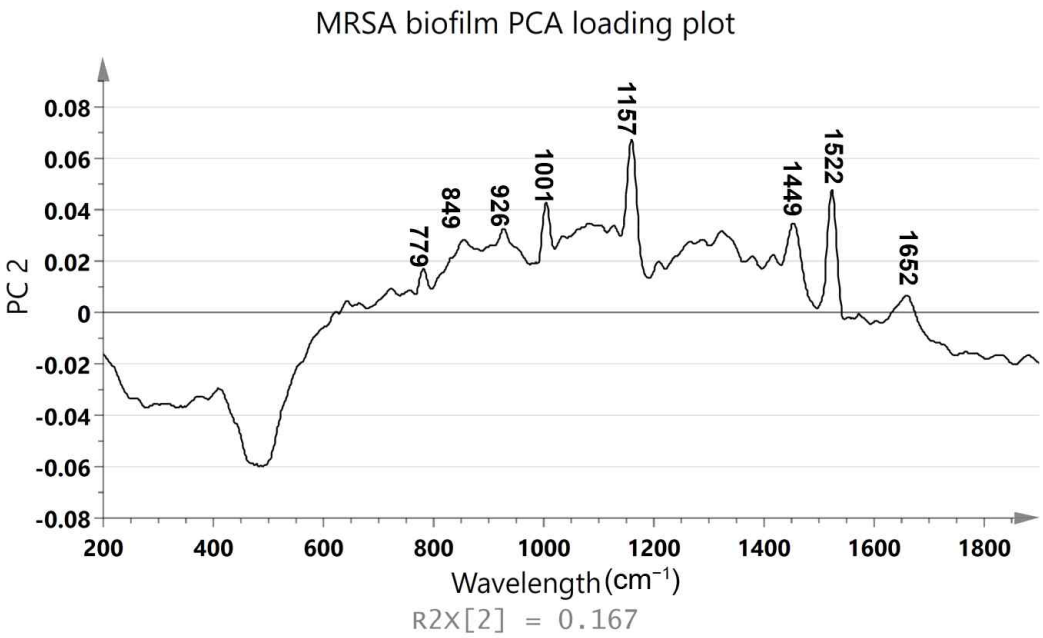

R2X[2] = 0.167

Figure 15. (a) Principal component analysis (PCA) was developed using the Raman spectra of methicillin-resistant Staphylococcus aureus (MRSA) biofilms with different cultivation times ranging from 0 - 48 h. N = 171, R2X(cum) = 0.97, Q2 (cum) = 0.99, Hotelling T2, 95% confidence level (the attachment phases (green), maturation phases (blue), and dispersal phases (red))are shown in PCA score plots. (b) Loading plot of the MRSA biofilm

As shown in Figure 13(b), biofilm growth stages were predicted based on spectral changes throughout the period. To confirm the prediction, PCA analysis was applied to the 171 spectral data. The Raman spectra of MRSA biofilms with different growth phases could be more clearly identified and visualized by performing PCA on the Raman spectra, as shown in Figure 15(a). PCA modeling was used to determine biomarkers that can discriminate biofilm growth phases and perform classification (Tarhan et al. 2021). A PCA analysis was performed to obtain an initial overview of the dataset and to detect trends. According to Hotelling T2 analysis, no samples were outside the 95% confidence ellipse. High values of explained variation (R2X = 0.97) and predictive ability Q2(cum) = 0.99 confirm the result of the analysis. In the PCA, approximately 97% of data variance is explained by the first two Principal components: PC1, and PC2. Fig. 3(a) shows the score plot of PC1, and PC2 of the growing MRSA biofilm, each of which accounts for 80.9%, and 16.7% of the variance, respectively. The data at different time points was demonstrated in three different groups to show the classification of biofilm states.

Figure 15(a) shows the PCA of Raman spectra for MRSA biofilms with different cultivation times ranging from 0 h to 48 h. The three different groups represent the different biofilm phases and display significant changes in Raman peak intensities and peak ratios. MRSA biofilms at three different metabolic states were clearly distinguished by the score plot. These three groups can be identified based on their time range on the score plot (0 - 5 h), corresponding to the

attachment of microbial cells at the first stage of biofilm formation (green); 6 – 24 h, corresponding to biofilm proliferation at the second stage (blue); and 26 – 48 h, corresponding to the dispersal of bacteria at the third stage (red). A separation of the group was better between the second (6 – 24 h) and third stages (26 – 48 h) (Figure 15(a)). Bacterial cells at the first stage overlapped slightly with biofilm colonies at the second stage. A poor group separation in the latter group of cell growth between the first and second stages indicates that there was an increasingly heterogeneous population of colonies at different growth stages, with some colonies reversibly and irreversibly attaching to surfaces. However, there is a clear seperation between the second and third stages of biofilms because the cells in the second stage still actively underwent metabolic changes, and in the third stage, metabolic cells were inactive. Principal component (PC) loadings provide information on variables (wavenumber of the spectrum) that are important for group separation. By analyzing these plots, one can indicate the most important variables in the dataset. The loading values of PCA are plotted in Figure 15(b). Based on these plots, it is possible to distinguish microorganisms by their unique metabolic activities. The analysis of the loading plot leads to the differentiation of important factors attributed to biofilm biomarkers depending on time. Using correlation coefficients (loadings) of component scores, spectral features important for biofilm phase discrimination were identified and their contributions to each variable were determined using PC. Instead, of examining a single

wavenumber peak, it is possible to do a more chemically rich analysis using regions of wavenumbers determined by correlation coefficients. It is more reliable to identify biomarkers that are important for discrimination when the selected spectral regions from loadings explain larger variances in data. Based on the loading plot, there was no significant contribution of growth changes in biofilm due at 481 cm^{-1}, which is a peak from monosaccharides of the medium. However, signature bands at 779, 926, 1002, 1159, 1247, 1342, 1457, 1525, and 1682 cm^{-1} showed high loading values. Especially, the hidden peak from 1682 cm^{-1} (amide I) was observed with a relatively high loading value by PCA. A significant intensity increase appeared for the amide I band of proteins at 1600 cm^{-1} after 26 h of incubation with biofilm accumulation. The increase in protein and lipid peaks indicates the stress response from biofilm growth (Keleştemur et al. 2017). An increase in protein concentration with increasing incubation time can be explained by the connection between protein expression and biofilm formation (Keleştemur et al. 2017). Based on PCA results, these Raman peaks demonstrate the most significant separation and absolute variances over time (Moritz et al. 2010). The loading peaks in PC are highly correlated to the activation of DNA/RNA formation at 600 - 800 cm^{-1} (Efeoglu et al. 2013). In second phase of the group, signature peaks of MRSA carotenoids and biofilm marker phenylalanine at 1002 and 1159 cm^{-1} are prominent (Wagner et al. 2009). Lastly, the peaks that differentiate the third phase of the biofilm are correlated to lipids and amides at 1400 - 1600

cm^{-1}, which are important components of EPS of biofilms (Chen et al. 2015). Figure 15(b) displays the most significant changes in spectral peaks during bacterial growth. Raman analysis can also be used to determine the metabolic state of unknown bacteria using these peaks (Moritz et al. 2010).

The results indicate that the PCA-based Raman technique can potentially identify and classify growing biofilm samples. The PCA method performed well in analyzing the Raman spectrum of growth of biofilm, and this analysis should be applicable in time-dependent antibiotic analysis. As a next step, a supervised analysis was conducted in the overlapping Phase 1 and Phase 2 to resolve metabolic variations. PLS-DA model was performed to classify the MRSA biofilm phases. The model was validated using a ROC curve and permutation testing.

3.4.3. PLS-DA plot to classify biofilm growth depending on spectral differences

In this research, PCA analysis gives a highly effective classification from initial planktonic cell to mature MRSA biofilm. Since planktonic bacterial cells are hard to distinguish from attached multicellular biofilm, PLS-DA was performed to find the correlation of the variables. The optimum number of latent variables is 8 in this study, and the method for estimating the latter number is k-fold cross validation. The explained variance in X and Y blocks, X is the wavelength of the Raman spectroscopy and Y variance biofilm phases. The class index matrix employed for training is class 1, and class 2. The class 1 includes from 1 to 53 sets that were classified as the first stage of biofilm in PCA analysis and the class 2 includes 117 sets of growth stage of biofilm. The statistical indicators of class prediction for the test set of samples RMSEE (root mean square estimated error) = 0.073, RMSE (root mean square error) cv = 0.093

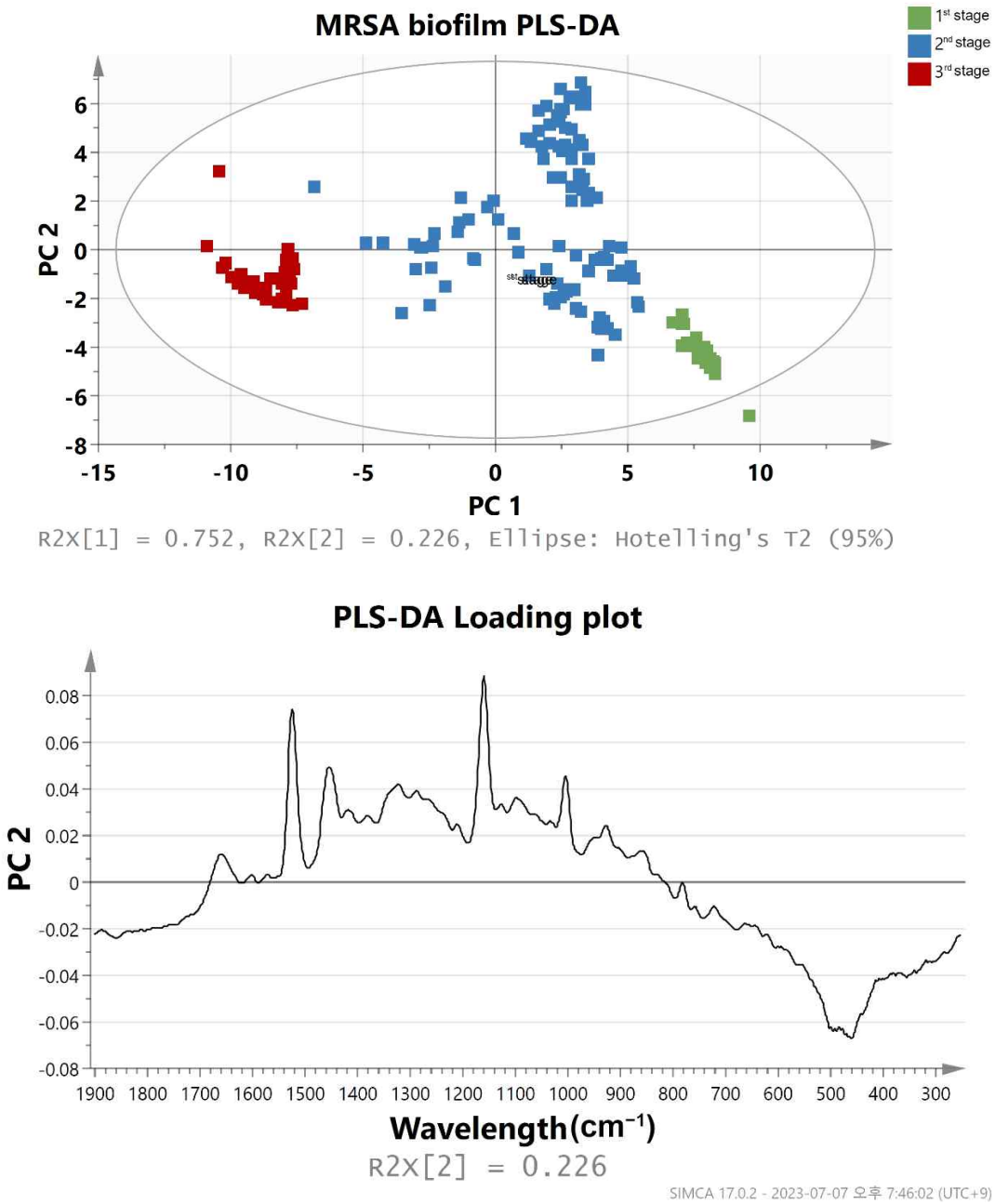

Figure 16.(a) PLS-DA scores plot (biofilm phases 1, 2, and 3) with A=1, N=170, R2X(cum)=0.97, R2Y(cum)=0.96, Q2(cum)=0.94 for Hotelling's T2 95% confidence level, p-value= 0 (b) Regression coefficient of component 1, R2X(2)=0.226.

In SIMCA-P, the quality of PLS-DA model was described by the goodness-of-fit R2 ($0 \leq R\ 2 \leq 1$) and the predictive ability Q2 ($0 \leq Q2 \leq 1$) values. An internal measure of model fit is provided by R2, and an internal measure of consistency to the cross-validation data is provided by Q2. In this study, PLS-DA models demonstrated high statistical values ($R2 > 0.7$ and $Q2 \geq 0.50$), the difference between the goodness-of-fit and the predictive ability always remained below 0.3 ($R2X(cum) - Q2\ (cum) < 0.3$) and the goodness of fit was never equal to one ($R2X(cum)\ 9= 0.98$). The cross-validation analysis of variance (CV-ANOVA) was used to validate the classification model, with a p-value < 0.05. Additionally, permutation tests were employed (500 permutations) in order to measure the effectiveness of the classification in a model by randomly permuting the original group attribution. All models were extracted at a confidence level of 95%. In this paper, the Receiver Operating Characteristics Curve (ROC) was drawn to validate the model. The area under the ROC curve equal to 1.

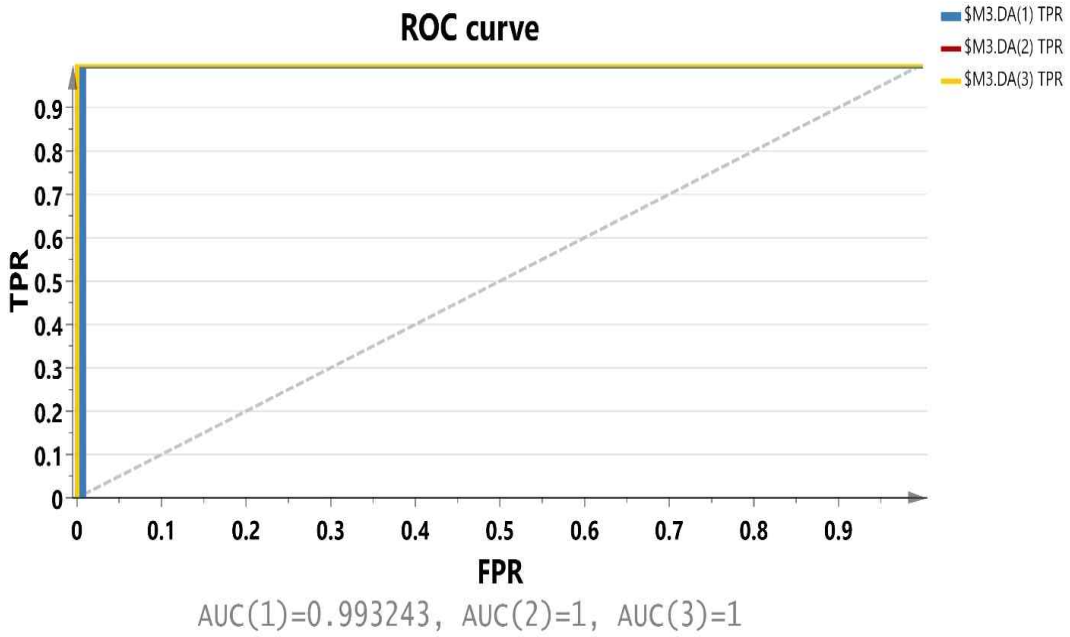

(a) Cross validation = ROC curve

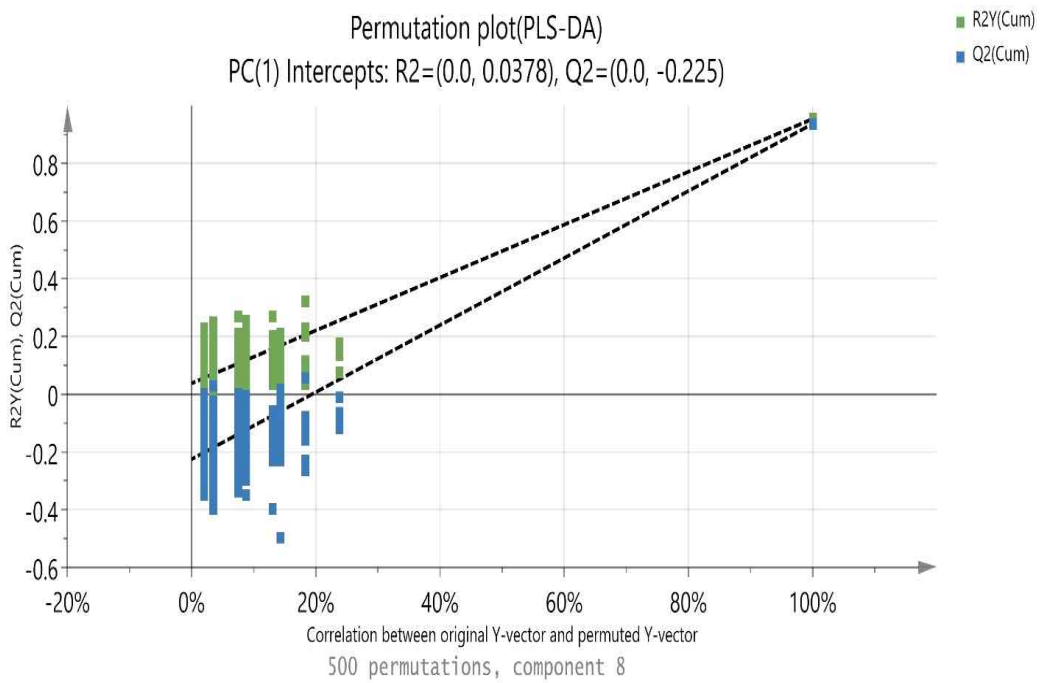

(b) Permutation plot (R2 = 0.0378, Q2=-0.225)

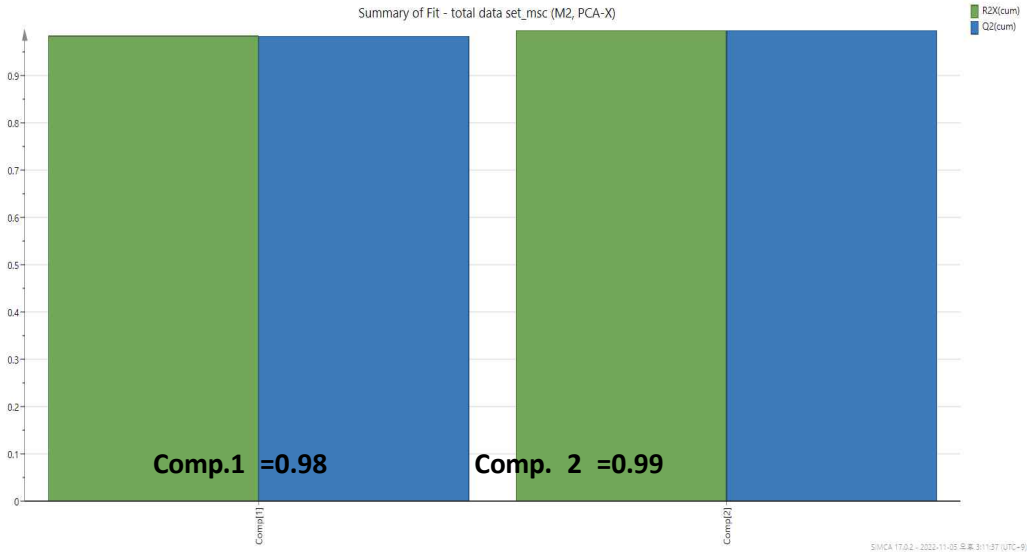

(c) Summary of fit

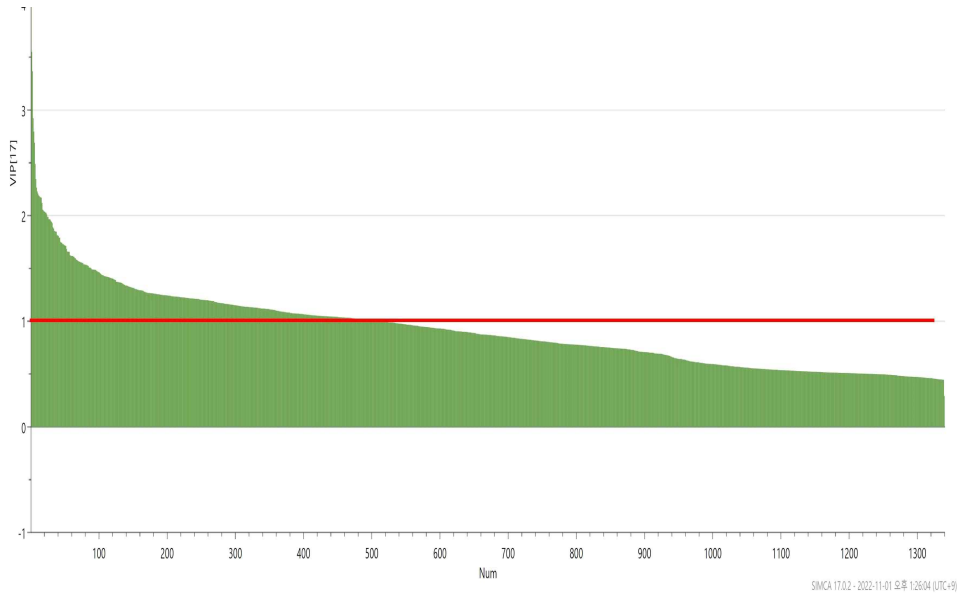

(d) VIP score

Figure 17. (a) ROC curve AUC (Phase 1) = 0.99 AUC (Phase 2) = 1 AUC (Phase 3) = 1. (B) Permutation test for the PLS-DA model.

M1	SS	DF	MS	F	p	SD
Total corr.	338	338	1			1
Regression	262.295	68	3.85728	13.7569	0	1.964
Residual	75.7048	270	0.280388			0.529517

Table 8. The cross-validation analysis of variance (CV-ANOVA) represented cross validation result, with a p-value = 0

These results were validated through cross validation. A VIP score is a measure of a variable's importance in the PLS-DA model. Variables in this model showed a VIP Score greater than 1 (one) that it can be considered important in this test.

3.4.4. Discrimination of biofilm growth by PLSR

PLSR is a modeling approach for the quantitative determination of bioactive components. The fundamental relationship of the Raman spectrum data and Colony forming unit values of biofilm were analyzed. As a result of performing regression analysis, the correlation coefficient was as high as R^2 = 0.97. This confirmed a strong correlation between Raman spectra and CFU/mL values. In the future, PLSR algorithm can be utilized if the modeling accuracy can be improved by standardizing the analysis conditions and increasing the number of samples.

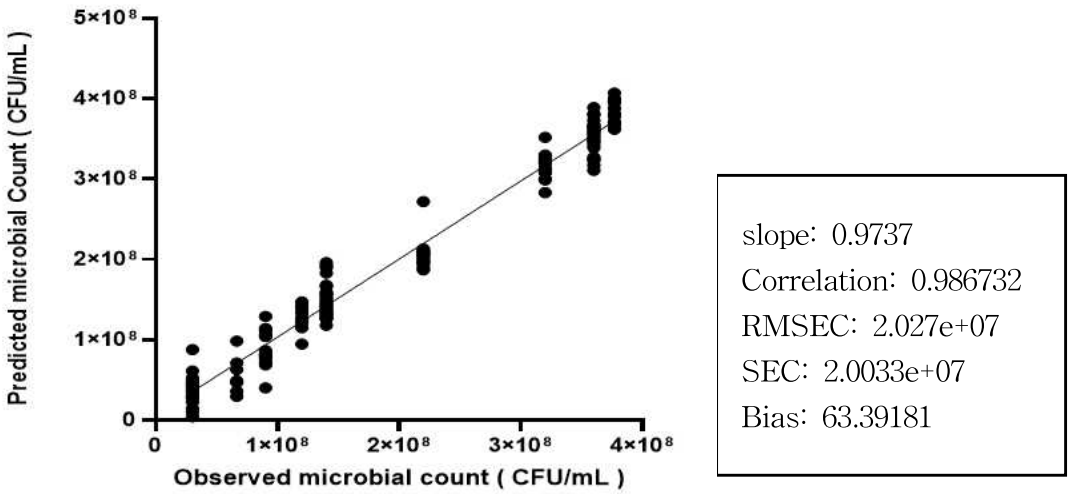

Figure 18. PLSR analysis of Raman spectra and microbial count (CFU/mL)

Chapter 4. Antimicrobial susceptible time of MRSA biofilm

4.1. Rapid antibiofilm test by Raman spectroscopy

4.1.1. Discrimination between biofilm vs. bacterial cell by Raman spectroscopy

To discriminate between the signals of biofilm cells from signals from planktonic cells, both spectra were analyzed by Raman spectroscopy. Interestingly, the signature peaks of the MRSA biofilm were marginal or absent at the beginning of biofilm growth (0 - 5 h). However, when the biofilm was grown for more than 4 hours, the signature peaks started to appear and helped to detect the formation of biofilm structure. In Figure 19, the mean spectrum of MRSA biofilm grown for 24 h was compared with that of planktonic bacteria cells incubated in the same conditions. In Smith-Palmer et al., the comparison of cytochrome C (CC) to phenylalanine (Phe) from Raman spectra was used to determine the growth of biofilm on surfaces. The CC peak is distinctive at approximately 780 cm^{-1} and the Phe is a sharp signal at 1004 cm^{-1}. Biofilm EPS has previously been found to contain CC, as identified by Raman microscopy. To compare the

proportions of EPS (CC) and protein (Phe) in a biofilm spectrum, the CC peak (747 cm^{-1}) and the Phe peak (1004 cm^{-1}) can be recorded. Further, the biofilm spectrum shows an intense peak at 1004 cm^{-1} associated with the ring breathing vibration of phenylalanine. Lastly, biofilm spectra differ significantly from those of planktonic cells, with signals related to a higher density of lipids at 1450 and 1334 cm^{-1}.

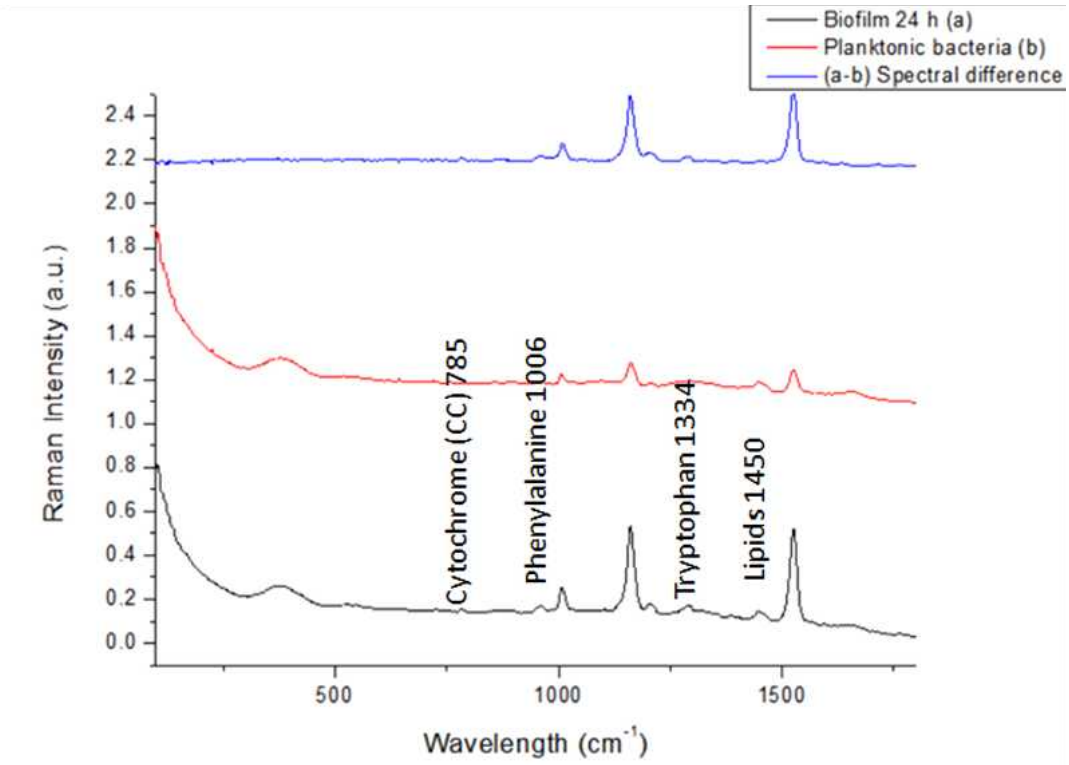

Figure 19. Mean Raman spectra of MRSA in mature biofilm grown for 24 h (A) and planktonic bacterial cells incubated under the same conditions are compared. The spectral difference (A - B) is shown in (C)

4.1.2. Proliferation abilities of MRSA biofilm after antibiotic treatments

In this research, the growth of MRSA biofilm was analyzed by PCA and the beginning of the proliferation stage starts after 5 hours of incubation. The optimizing time to eradicate biofilm is during the attachment stage (0 - 5 h) and it was validated through the characterization of eugenol-MRSA biofilm interaction using microbiological methods. Since eugenol is known to demonstrate strong anti-biofilm properties against both MRSA and MSSA clinical strains, it was selected as a natural biofilm agent for rapid anti-biofilm tests (Yadav et al. 2015). Anti-biofilm assay was performed to determine the antibacterial activity of eugenol on MRSA within the biofilms. Biofilms exposed to 2 × MIC displayed strong bactericidal effects against MRSA (Yadav et al. 2015). After the treatment on 5 h grown biofilm, counts of viable bacterial cells were decreased by more than 2-$\log_{10}$ and 4-$\log_{10}$. This observation suggests that the strong bactericidal activity of eugenol on MRSA within biofilms reaches maximal effect toward 0 - 5 h grown biofilm. The result is in agreement with the prediction.

In parallel to the anti-biofilm assay, antibiotics on cell viability were tested in MBHI agar plate with the same inoculum and reagents for Raman experiments.

To figure out when spectral changes occur, each time point was compared individually by Raman spectroscopy. Eugenol at MIC was

applied to monitor its killing effect on biofilms at different stages.

From the experiment, biofilm stages could be divided into three steps, and the difference between the attachment and dispersal stages of biofilms could be observed in the pattern changes to further verify the correlation of antimicrobial activity on biofilms. In Figure 19, MRSA biofilms in the attachment stage (approximately 5 h) were treated with eugenol, and changes in the Raman spectrum were observed. The bands at 764, 1280, 1334, 1450, 1526, and 1650 cm^{-1} significantly decreased after the antibiotic treatment. The peaks were correlated to DNA/RNA fragments, tryptophan, lipid, carotenoid, and amide of MRSA biofilms. The significant decrease in the Raman spectrum in the attachment stage indicates that the antibiotic effect on MRSA biofilms is very high in the initial phase, making it the most optimal time to apply antibiotic agents. In the dispersal stage (36 h) shows that the peak at 652 cm^{-1} was decreased under eugenol treatment. Despite the overall decrease in Raman intensities, the peaks were not disrupted by eugenol application. Based on the Raman spectra monitoring the eugenol-treated biofilms at different times, the biofilm at the dispersal stage showed less disruption than those at the attachment stage. Consequently, Raman spectroscopy could predict the best time for antimicrobial activity against MRSA biofilms by observing the spectral changes in the Raman spectrum of bacterial cells.

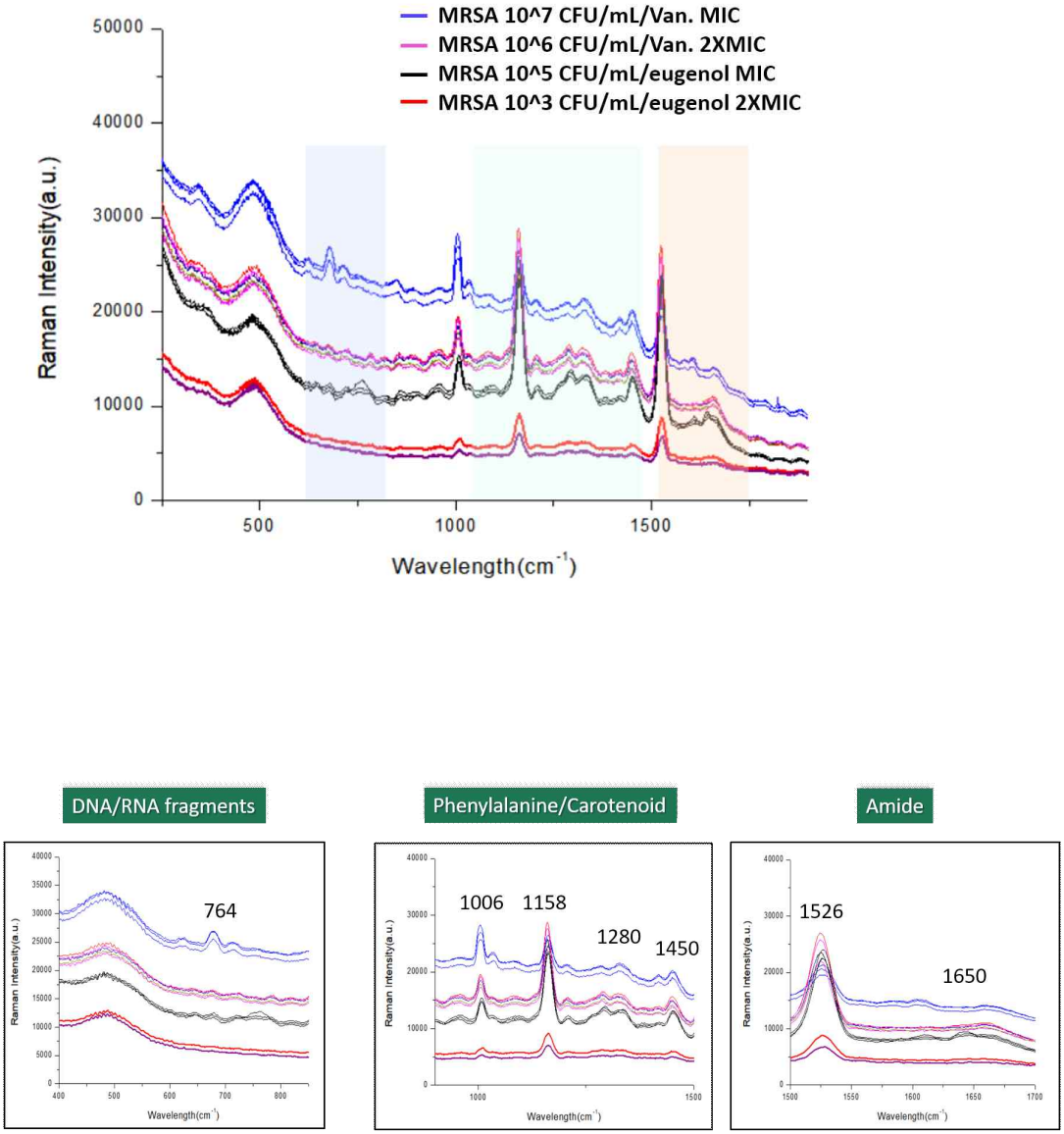

Figure 20. Raman spectra of methicillin-resistant Staphylococcus aureus biofilms at the attachment stage and biofilm with eugenol treatment at minimum inhibitory concentrations.

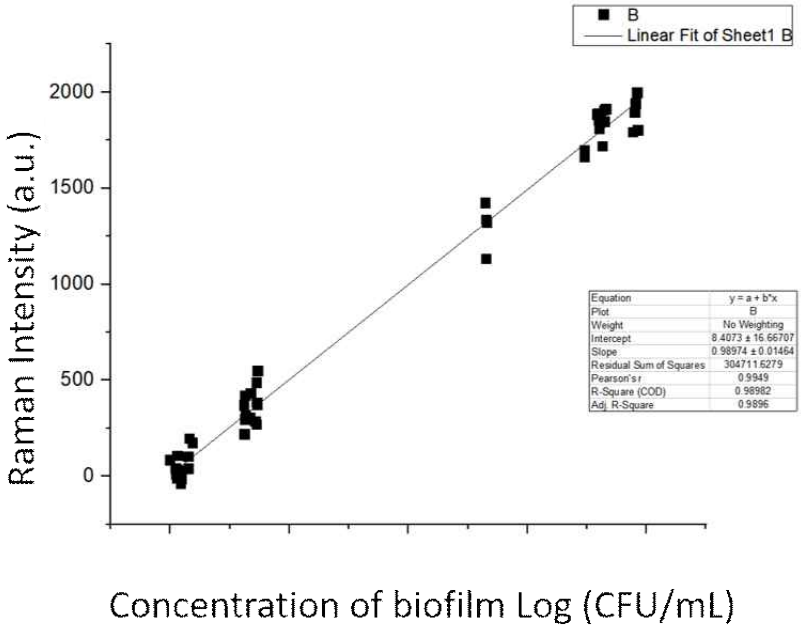

Figure 21. Correlation between Raman intensity and concentration of biofilm (CFU/mL)

In Figure 20, Raman shifting was examined in different metabolites of biofilm. The DNA/RNA fragments, vanished after the antimicrobial treatment. The biofilm characteristic phenylalanine and carotenoid reduced significantly. Interestingly, at eugenol MIC concentration did not influence the Lipid peaks but at MBIC concentration, the peaks faded. Lastly, at amide peaks at 1650 cm^{-1} were not affected at both vancomycin and eugenol MIC concentration. However, at MBIC concentration, both showed reducing of the band. In parallel to the raman analysis, the antibiotics on cell viability were tested to quantify the antibiofilm test.

4.1.3. Determining the antibacterial activity of eugenol based on cell counts in biofilms

A biofilm is a dominant form of microbial life, and it is difficult to eliminate it completely. It provides protection to residing bacteria, so it is critical to find the best antibiotics in the most effective time frame. Therefore, the best time to apply eugenol was examined by Raman spectroscopy (Figure 19). According to CFU calculations, in Figure 21 the number of biofilms counted was in agreement with the above results. In Figure 22, the CFU was calculated on 3M petrifilm. Eugenol demonstrated anti-biofilm properties against clinical MRSA strains, especially in the early phase of biofilm formation. The biomasses of established biofilms were significantly decreased by eugenol treatment. Similarly, the number of viable bacteria was significantly decreased in eugenol-treated biofilms. Biofilm biomass was significantly decreased by 50% when eugenol was applied at MIC (Yadav et al. 2015). A decrease 4-$\log_{10}$ in the number of viable cells was observed in biofilms treated with eugenol at 2×MIC. The MBC of eugenol against MRSA biofilms was found to be twice its MIC value (Uppu et al. 2017).

The antibacterial activities of eugenol were investigated against MRSA. Eugenol was evaluated for bactericidal activity by counting viable cells, providing a quantitative estimate of its efficacy. The inhibitory activities of eugenol and vancomycin are shown in Figure 21. The samples were enumerated for bacterial viability at 24 h of

exposure to the antibiotics. The proliferation abilities of bacterial cells after treatment with the selected antibiotics at one and two times the MIC on biofilms at different stages are shown in Fig. 5. When MRSA biofilms grown for 36 h were exposed to eugenol at MIC, no significant difference was observed in the proliferation ability of MRSA. At two times the MIC, 7.3 logs CFU/mL bacterial cells could proliferate, and at MIC, 8.5 logs CFU/mL bacterial cells lived. However, the proliferation ability of MRSA biofilms decreased sharply when only grown for <5 h and treated with eugenol. After the antibiotic treatment, growing biofilms showed 4.3 logs CFU/mL cells at two times the MIC and 5.7 logs CFU/mL cells at MIC. Similarly, 6.8 logs CFU/mL was observed for vancomycin treatments (Fig. 5). Based on these findings, treatment with eugenol at an early stage of biofilm formation could enhance its bactericidal effects. To get further insights into the correlation between Raman spectral changes with antimicrobial activities to biofilm at different stages, PCA was used. This study showed that the results from antibacterial activity were in good agreement with those from PCA, making the method useful to determine the optimum time for antibiotic administration.

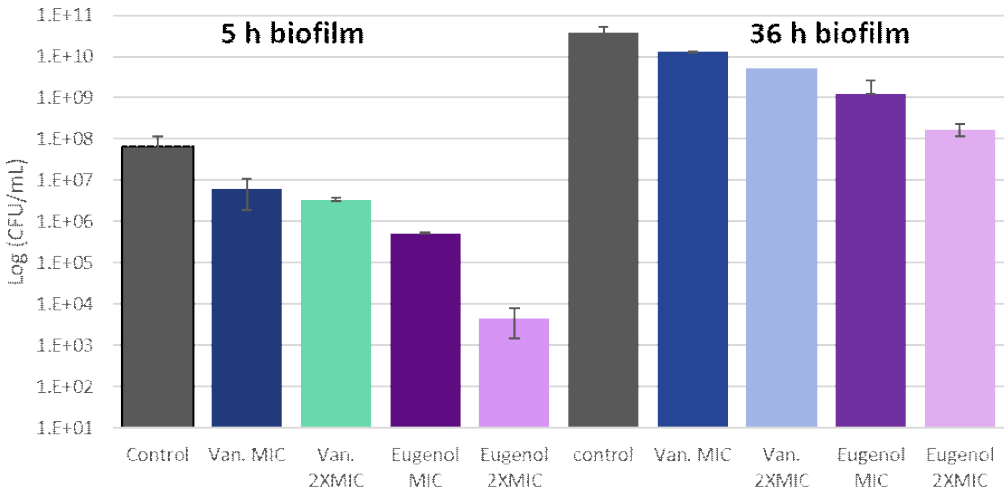

Figure 22. Quantitative analysis of the antibacterial activity of the eugenol-loaded composites by direct contact, for 5 and 36 hours, against MRSA.

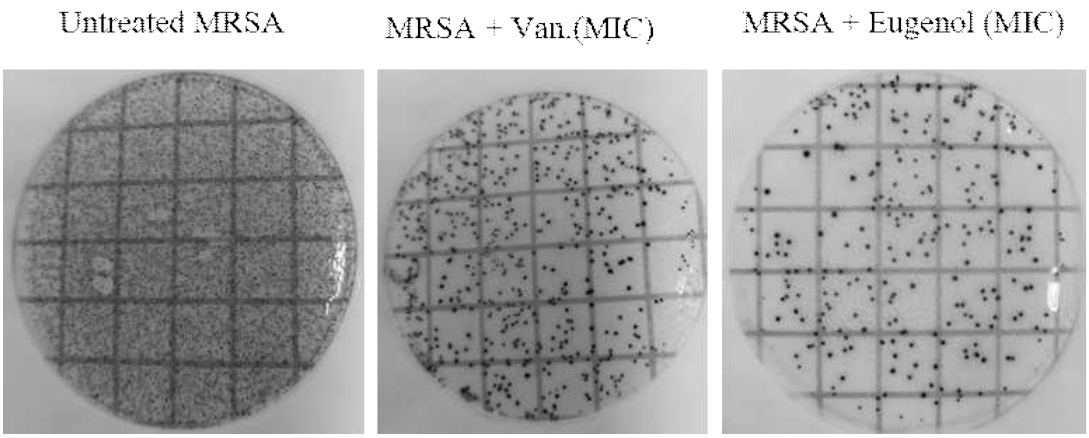

Figure 23. Petrifilm result of MRSA CFU/mL

4.1.4. Prospects and Challenges

Raman spectroscopy can be used to analyze instantaneously the chemical properties of MRSA biofilms. It can compensate for traditional approaches such as CRA assays and crystal violet assays that permanently dye bacterial cells. Although the tool has advantages, the study still has limitations. The micro-scale analysis of Raman spectroscopy makes it difficult to capture the large range of complexity in biofilms. Since Raman spectroscopy is limited by the size of the sample, only a certain amount of material can be analyzed at a time. This means that only a small section of the biofilm can be studied. The Raman mapping is shown in Figure 10a to overcome this limitation. By combining the micro-scale analysis of Raman spectroscopy with Raman mapping, it was possible to capture the large range of complexity in biofilms. This technique is used to produce detailed chemical images of samples and can analyze be used to larger samples than can be analyzed via traditional Raman spectroscopy. Another challenge in the study was the limited number of bacteria samples. The study would have been more relevant to the broader range of microbes if more than one strain was used. Research using various strains can help determine which factors influence the microbial population and biofilm health. Additionally, comparing multiple strains gives a better understanding of how different microbes interact with each other and affect the biofilm. To

ensure a more accurate representation of the microbial population, multiple bacterial strains should be studied in future research. Additionally, the study could have been improved by conducting more than one antibiotic agent efficacy assessment. This would have allowed for a better understanding of the effectiveness of the antibiotic agents. Additionally, the results would have been more reliable and comprehensive. We are planning to perform a screening of natural compounds on biofilms at different growth stages using Raman spectroscopy for further study. Despite the challenges to this research, Raman spectroscopy was advantageous to analyzing biological samples. For example, it allowed for a non-invasive and label-free approach to the analysis of biofilms and could provide information about the composition of the biofilm, changes in the biofilm over time, and the effect of drugs on the biofilm. Furthermore, Raman spectroscopy has the potential to provide insight into biological processes that would be difficult to access with traditional methods.

Chapter 5. Conclusion

In this study, a novel approach was presented using Raman spectroscopy to identify new, safe, and effective agents with which to combat the increasing number of multi-resistant strains of bacteria. As MRSA forms a biofilm, the resistance against antibiotics increased and the natural compound eugenol was tested to inhibit the bacteria. There are several methods to evaluate bacteria, including crystal violet assays, Congo red agar assays, and SEM analysis. However, staining bacterial cells permanently can impact their functionality. In addition, it can be difficult to distinguish between different types of bacteria under the microscope, and results can be subjective. As a result, traditional staining techniques may not always be the best option for bacterial evaluation. Alternatively, Raman spectroscopy can be an effective option. It only takes a few minutes for the analysis to be completed, allowing the real-time monitoring of the results. This method allowed for a more accurate assessment of the biofilm structure as no staining or processing was required. Furthermore, it is a non-destructive technique, meaning that bacterial cells remain intact and functional. As a result, Raman spectroscopy can be used to predict initial MRSA biofilm adhesion to the surface and the optimal antibiotic administration time to avoid resistance caused by biofilm formation. Biofilm growth was examined by measuring the changes

in the Raman spectrum of biofilms and primary matrix materials, such as DNA, RNA, protein, lipid, and EPS. When analyzing the measured Raman spectrum changes using PCA, PLS-DA, and PLSR three different biofilm growth stages were confirmed. To predict the optimal antibiotic administration stage during biofilm formation, eugenol was treated at 5 h, 24 h, and 36 h. The most effective biofilm growth could be inhibited when treated before 5 h, and this result was consistent with the results based on quantified biofilm mass(CFU/mL). Based on this study, Raman spectroscopy could be used to measure real-time biofilm formation without staining and suggest the optimal time for antibiotic administration to prevent biofilm formation.

References

D. S. Abbanat, W. Amsler, K. Santoro, C. Baum, E. Crespo-Carbone, S. Lynch, Evaluation of the in vitro activities of ceftobiprole and comparators in staphylococcal colony or microtitre plate biofilm assays, Int. J. Antimicrob. Agents. 43(1) (2014) 32-39,

S. Stöckel, J. Kirchhoff, U. Neugebauer, P. Rösch, J. Popp, The application of Raman spectroscopy for the detection and identification of microorganisms, J. Raman. Spectrosc. 47(1)

N. N. Wickramasinghe, M. M. Hlaing, J, T. Ravensdale, R. Coorey, P. S. Chandry, G. A. Dykes, Characterization of the biofilm matrix composition of psychrotrophic, meat spoilage pseudomonads, Sci. Rep. 10(1) (2020) 16457,

T. Verma, H. Annappa, S. Singh, S. Umapathy, D. Nandi, Profiling antibiotic resistance in Escherichia coli strains displaying differential antibiotic susceptibilities using Raman spectroscopy, J. Biophotonics. 14(1) (2021) e202000231-n/a.

G. O'Toole, H. B. Kaplan, R. Kolter, Biofilm formation as microbial development, Annu. Rev. Microbiol. 54 (2000) 49-79.

K. Sauer, A. K. Camper, G. D. Ehrlich, J. W. Costerton, D. G. Davies, Pseudomonas aeruginosa displays multiple phenotypes during development as a biofilm, Annu. Rev. Microbiol. 184(4) (2002) 1140-1154

A. W. Smith, Biofilms and antibiotic therapy: Is there a role for combating bacterial resistance by the use of novel drug delivery systems? Adv. Drug Deliv. Rev. 57(10) (2005) 1539-1550

A. Bagheri Pebdeni, M. Hosseini, Fast and selective whole cell detection of Staphylococcus aureus bacteria in food samples by paper based colorimetric nanobiosensor using peroxidase-like catalytic activity of DNA-Au/Pt bimetallic nanoclusters, Microchem. J. 159 (2020) 105475

M. Zareef, M. Mehedi Hassan, M. Arslan, W. Ahmad, S. Ali, Q. Ouyang, H. Li, X. Wu, Q. Chen, Rapid prediction of caffeine in tea based on surface-enhanced Raman spectroscopy coupled multivariate calibration, Microchem. J. 159 (2020) 105431

L. Cui, D. Zhang, K. Yang, X. Zhang, Y. G. Zhu, Perspective on surface-enhanced Raman spectroscopic investigation of microbial world, Anal.Chem. 91(24) (2019) 15345-15354

N. P. Ivleva, M. Wagner, H. Horn, R. Niessner, C. Haisch, Towards a nondestructive chemical characterization of biofilm matrix by Raman microscopy, Anal. Bioanal. Chem. 393(1) (2009) 197-206

M. B. Jabłoński, E. A. Stefaniak, L. Darchuk, K. Turżańska, M. Gorzelak, R. Kuduk, W. Dorriné, R. Van Grieken, Microchemical investigation of bone derived from mice treated with strontium in different chemical forms using scanning electron microscopy and micro-Raman spectroscopy, Microchem. J. 108 (2013) 168-173

O. Samek, K. Mlynariková, S. Bernatová, J. Ježek, V. Krzyžánek, M. Šiler, P. Zemánek, F. Růžička, V. Holá, M. Mahelová, Candida parapsilosis biofilm identification by Raman spectroscopy, Int. J. Mol. Sci. 15(12) (2014) 23924-23935

L. C. Lee, A. A. Jemain, On overview of PCA application strategy in processing high dimensionality forensic data, Microchem. J. 169 (2021) 106608

M. R. Almeida, C. H. Fidelis, L. E. Barata, R. J. Poppi, Classification of Amazonian rosewood essential oil by Raman spectroscopy and PLS-DA with reliability estimation, Talanta 117 (2013)

305-311

I. Tarhan, I. Işık, B. Söğüt, Application of ATR-FTIR spectroscopy in tandem with chemometrics for assessing the firing conditions of Hellenistic and Roman ceramic shards excavated from the ancient city of Stratonikeia in South-Western Turkey, Microchem. J. 162 (2021) 105852

M. Oravec, K. Haberová, K., V. Jančovičová, Z. Machatová, M. Čeppan, C. W. Huck, Identification of the historic photographic print materials using portable NIR and PCA, Microchem. J. 150 (2019) 104202

G. Jell, I. Notingher, O. Tsigkou, P. Notingher, J. M. Polak, L. L. Hench, M. M. Stevens, Bioactive glass-induced osteoblast differentiation: A noninvasive spectroscopic study, J. Biomed. Mater. Res. A 86(1) (2008) 31-40

K. Maquelin, L.-P. i. Choo-Smith, T. van Vreeswijk, H. P. Endtz, B. Smith, R. Bennett, H. A. Bruining, G. J. Puppels, Raman Spectroscopic Method for Identification of Clinically Relevant Microorganisms Growing on Solid Culture Medium, Anal. Chem. 72(1) (2000) 12-19

H. Shen, P. Rösch, J. Popp, Fiber Probe-Based Raman Spectroscopic

Identification of Pathogenic Infection Microorganisms on Agar Plates, Anal. Chem. 94(11) (2022) 4635-4642

A. O. H. Gill, R. A. Holley, Mechanisms of bactericidal action of cinnamaldehyde against Listeria monocytogenes and of eugenol against L. Monocytogenes and Lactobacillus sakei, Appl. Environ. Microbiol. 70(10) (2004) 5750-5755

S. Hashimoto, K. Uchiyama, M. Maeda, K. Ishitsuka, K. Furumoto, Y. Nakamura, In vivo and in vitro effects of zinc oxide-eugenol (ZOE) on biosynthesis of cyclo-oxygenase products in rat dental pulp, J. Dent. Res. 67(8) (1988) 1092-1096

M. J. A.-B. Mohammed, F. A. Al-Bayati, Isolation and identification of antibacterial compounds from Thymus kotschyanus aerial parts and Dianthus caryophyllus flower buds, Phytomedicine 16(6-7) (2009) 632-637

S. E. K. Moon, H. Y. Kim, J.D., J. D. Cha, Synergistic effect between clove oil and its major compounds and antibiotics against oral bacteria, Arch. Oral Biol. 56(9) (2011) 907-916

M. K. Yadav, S. W. Chae, G. J. Im, J. W. Chung, J. J. Song, Eugenol: A phyto-compound effective against methicillin-resistant and methicillin-sensitive Staphylococcus

aureus clinical strain biofilms, PLoS One. 10(3) (2015) e0119564

I. Raad, R. Darouiche, R. Hachem, M. Sacilowski, G. P. Bodey, Antibiotics and prevention of microbial colonization of catheters, Antimicrob. Agents Chemother. 39(11) (1995) 2397-2400

D. J. F. Freeman, F. R. Falkiner, C.T., C. T. Keane, New method for detecting slime production by coagulase negative staphylococci, J. Clin. Pathol. 42(8) (1989) 872-874

N. M. T. Jebril, Evaluation of two fixation techniques for direct observation of biofilm formation of Bacillus subtilis in situ, on Congo red agar, using scanning electron microscopy, Vet. World 13(6) (2020) 1133-1137

O. Taofiq, S. A. Heleno, R. C. Calhelha, I. P. Fernandes, M. J. Alves, L. Barros, A. M. González-Paramás, I. C. F. R. Ferreira, M. F. Barreiro, Phenolic acids, cinnamic acid, and ergosterol as cosmeceutical ingredients: Stabilization by microencapsulation to ensure sustained bioactivity, Microchem. J. 147 (2019) 469-477

D. S. S. M. Uppu, M. M. Konai, P. Sarkar, S. Samaddar, I. C. M.

Fensterseifer, C. Farias-Junior, P. Krishnamoorthy, B. R. Shome, O. L. Franco, J. Haldar, Membrane-active macromolecules kill antibiotic-tolerant bacteria and potentiate antibiotics towards Gram-negative bacteria, PLoS One 12(8) (2017)

CLSI. Performance standards for antimicrobial susceptibility testing (28th edition). CLSI supplement M100: M100-S22. Clinical and Laboratory Standards Institute, PA, USA (2018)

K. Silbernagel, R. Jechorek, C. Carver, B. Horter, K. Lindberg, V. Aleo, G. Anderson, B. Bannach, M. Bulthaus, K. Chaemcheun, K. Dixon, B. Hemming, M. Iannucci, A. Johnson, K. Johnson, A. Kaufer, S. Kemp, J. King, C. Xiong, 3MTM PetrifilmTM staph express count plate method for the enumeration of Staphylococcus aureus in selected dairy foods: Collaborative study, J. AOAC Int. 86(2003) 963-970

P. S. Panda, U. Chaudhary, S. K. Dube Comparison of four different methods for detection of biofilm formation by uropathogens, Indian. J. Pathol. Microbiol. 59(2) (2016) 177-179,

V. K. Moses, V. Kandi, S. K. D. Rao, Minimum inhibitory concentrations of vancomycin and daptomycin against methicillin-resistant Staphylococcus aureus isolated from

various clinical specimens: A study from South India, Cureus 12(1) (2020) e6749

P. C. Chen, L. Cui, K. Zhang, Surface-enhanced Raman spectroscopy monitoring the development of dual-species biofouling on membrane surfaces, J. Membr. Sci. 473(2015) 36-44

E. C. Efeoglu, M. Culha, In situ-monitoring of biofilm formation by using surface-enhanced Raman scattering, Appl. Spectrosc. 67(5) (2013) 498-505

Y. X. Xie, L. Wang, Y. Shao, J. Wang, L. Wang, Heya Qian, W. He Yao, Label-free detection of the foodborne pathogens of Enterobacteriaceae by surface-enhanced Raman spectroscopy, Anal. Methods. 5(4) (2013) 946-952

P. Kao, N. A. Malvadkar, M. Cetinkaya, H. Wang, D. L. Allara, M. C. Demirel, Surface-enhanced Raman detection on metalized nanostructured poly(p-xylylene) films, Adv. Mater. 20(18) (2008) 3562-3565

R. M. Jarvis, A. Brooker, R. Goodacre, Surface-enhanced Raman spectroscopy for bacterial discrimination utilizing a scanning electron microscope with a Raman spectroscopy interface, Anal. Chem. 76(17) (2004) 5198-5202,

L. Cui, B. Liu, D. Vonlanthen, M. Mayor, Y. Fu, J. F. Li, T. Wandlowski, In situ gap-mode Raman spectroscopy on single-crystal Au(100) electrodes: Tuning the torsion angle of 4,4'-Biphenyldithiols by an electrochemical gate field, J. Am. Chem. Soc. 133(19) (2011) 7332-7335

M. Wagner, Single-cell ecophysiology of microbes as revealed by Raman microspectroscopy or secondary ion mass spectrometry imaging, Annu. Rev. Microbiol. 63(1) (2009) 411-429

A. C. S. Talari, Z. Movasaghi, S. Rehman, Iu Rehman, Raman spectroscopy of biological tissues, Appl. Spectrosc. Rev. 50(1) (2015) 46-111.

X. Yang, C. Gu, F. Qian, Y. Li, J. Z. Zhang, Highly sensitive detection of proteins and bacteria in aqueous solution using surface-enhanced Raman scattering and optical fibers, Anal. Chem. 83(15) (2011) 5888-5894

K. C. Schuster, E. Urlaub, J. R. Gapes, Single-cell analysis of bacteria by Raman microscopy: Spectral information on the chemical composition of cells and on the heterogeneity in a culture, J. Microbiol. Methods. 42(1) (2000) 29-38

A. Manilal, K. R. Sabu, M. Shewangizaw, A. Aklilu, M. Seid, B. Merdikios, B. Tsegaye, In vitro antibacterial activity of medicinal plants against biofilm-forming methicillin-resistant Staphylococcus aureus: Efficacy of Moringa stenopetala and Rosmarinus officinalis extracts, Heliyon 6(1) (2020) e03303

J. Sundaram, B. Park, Y. Kwon, K. C. Lawrence, Surface enhanced Raman scattering (SERS) with biopolymer encapsulated silver nanosubstrates for rapid detection of foodborne pathogens, Int. J. Food Microbiol. 167(1) (2013) 67-73

L. Xue, Y. Y. Chen, Z. Yan, W. Lu, D. Wan, H. Zhu, Staphyloxanthin: A potential target for antivirulence therapy, Infect. Drug Resist. 12(2019) 2151-2160

O. D. Ayala, C. A. Wakeman, I. J. Pence, J. A. Gaddy, J. C. Slaughter, E. P. Skaar, A. Mahadevan-Jansen, Drug-resistant Staphylococcus aureus Strains Reveal distinct biochemical features with Raman microspectroscopy, ACS Infect. Dis. 4(8) (2018) 1197-1210

K. Rebrošová, M. Šiler, O. Samek, F. Růžička, S. Bernatová, J. Ježek, P. Zemánek, V. Holá, Identification of ability to form biofilm in Candida parapsilosis and Staphylococcus epidermidis by

Raman spectroscopy, Future Microbiol. 14 (2019) 509-517

L. Wang, W. Liu, J. W. Tang, J. J. Wang, Q. H. Liu, P. B. Wen, M. M. Wang, Y. C. Pan, B. Gu, X. Zhang, Applications of Raman spectroscopy in bacterial infections: Principles, advantages, and shortcomings, Front. Microbiol. 12 (2021) 683580

C. Ebert, L. Tuchscherr, N. Unger, C. Pöllath, F. Gladigau, J. Popp, B. Löffler, U. Neugebauer, Correlation of crystal violet biofilm test results of Staphylococcus aureus clinical isolates with Raman spectroscopic read-out, J. Raman Spectrosc. 52(12) (2021) 2660-2670

W. H., R. Nelson, Manoharan, J. F. Sperry, UV resonance Raman studies of bacteria, Appl. Spectrosc. Rev. 27(1) (1992) 67-124

Y. Ren, Y. Ji, L. Teng, H. Zhang, Using Raman spectroscopy and chemometrics to identify the growth phase of Lactobacillus casei Zhang during batch culture at the single-cell level, Microb. Cell Fact. 16(1) (2017) 233-233

A. E. H. Paharik, A. R. Horswill, The staphylococcal biofilm: Adhesins, regulation, and host response, Microbiol. Spectr. 4(2) (2016)

T. J. Moritz, D. S. Taylor, C. R. Polage, D. M. Krol, S. M. Lane, J. W. Chan, Effect of cefazolin treatment on the nonresonant Raman signatures of the metabolic state of individual Escherichia coli Cells, Anal. Chem. 82(7) (2010) 2703-2710

B. G. Botelho, N. Reis, L. S. Oliveira, M. M. Sena, Development and analytical validation of a screening method for simultaneous detection of five adulterants in raw milk using mid-infrared spectroscopy and PLS-DA, Food Chem. 181 (2015) 31-37

M. Hoehse, A. Paul, I. Gornushkin, U. Panne, Multivariate classification of pigments and inks using combined Raman spectroscopy and LIBS, Anal. Bioanal. Chem. 402(4) (2012) 1443-1450

S. Ç. Keleştemur, M. Çulha, Understanding and discrimination of biofilms of clinically relevant microorganisms using surface-enhanced Raman scattering, Appl. Spectrosc. 71(6) (2017) 1180-1188,

국문초록

라만 분광학을 이용한 메틸실린 내성 포도상구균 바이오필름 성장 실시간 모니터링 연구

서울대학교 대학원
약학과 생약학전공
김지나

전 세계적으로 항균제 내성 박테리아의 확산은 중요한 도전 과제가 되었다. 메티실린 내성 황색포도상구균 (MRSA) 감염은 고분자 의료 기기 및 임플란트에 생물막을 형성하여 항생제에 대한 내성을 약 1,000배 가까이도 증가시킨다. 이러한 항생제 내성 및 생체막 형성 문제로 새로운 항균제와 대체요법이 시급하다. 특히, 항균제의 투여시간이 생물막 근절에 직접적인 영향이 있음이 밝혀져 효과적인 항균제를 적절한 생물막 성장 시기에 적용하는 것이 중요하다. 바이오필름이 생체 내 약물 내성 발달에 중요 하다는 점을 고려할 때, 바이오필름에 대한 약물의 효과를 평가하는 효과적인 방법이 필요하다. 이를 보완하기 위하여 MRSA 생물막의 성장과정을 모니터링하고 단계별 항균 효과를 측정하기 위하여 라만 분광법을 수행하였다.

라만 분광법은 레이저가 분자의 공명에 의해 산란되는 특성을 이용하여 세포 내 지질, 핵산, 단백질 등의 구성물질을 신속하게 측정할 수 있어 세균 검측에 적합한 기술로 알려져 있다. 세포 구성물질에 대한 높은

특이성과 민감성 때문에 라만 스펙트라(spectra)만으로 생리적 활성 변화에 대한 정량이나 정성 평가에 활용할 수 있다. 본 연구에서는 신속하게 라만 분광기로 균주 생물막의 성장을 정성 정량 분석하여 최적의 항균제 투여시기를 알아보는 플랫폼을 개발하고자 하였다.

MRSA 생물막을 0시간에서 48시간 동안 라만 분광기로 측정하였다. MRSA 생물막 배양 첫 5시간 동안 배지의 주성분인 단당류는 495 cm^{-1}에서 라만 신호를 생성했다. 6~24시간 후, DNA/RNA와 상관관계가 있는 764, 1012, 1159 및 1526 cm^{-1} 피크가 증가하고 생물막의 케로티노이드가 증가하여 박테리아 부착 및 증식이 발생을 확인했다. 배양 25-48시간 동안 DNA/RNA 관련 신호는 감소하고 1440-1460 및 1630 cm^{-1}이 증가하여 EPS의 변화가 일어남을 확인하였다. 생물막의 주성분 분석을 통하여 MRSA 성장의 3가지 다른 단계를 식별하였다.

48시간 동안 모니터링을 통하여 171개의 라만 스펙트럼을 얻을 수 있었다. 많은 데이터의 분류와 상관관계를 알아내기 위하여 다변량분석법(PCA, PLS-DA, PLSR)을 사용하여 바이오필름의 성장과정을 스테이지별로 구분 지어 봤다. 이 중 가장 항균 효과가 큰 시점을 찾기 위하여 생물막 감수성 확인을 라만 분광기로 수행하였다. 확인한 결과는 CFU(Colony Forming Unit) 결과로 효용성을 같이 입증하였습니다.

MRSA 생물막의 항균 활성을 확인하기 위하여 항균제 감수성 검사를 통하여 총 11개의 생약성분 중 유제놀의 유의미한 항균효과를 확인하였다. 기존에는 유제놀에 대한 일부 약효에 대한 연구는 있었으나 실제 임상 균주의 생물막을 대상으로 한 연구결과는 아직까지 없다. 생물막 억제 과정을 확인하기 위하여 유제놀을 항균제로 선정하였다. 유제놀은 정향(Caryophilli Flos, Myrtaceae)의 주성분으로 현재 국소마취제로 이용되거나, 자궁수축, 항진균, 항바이러스 효과 억제한다는 보고가 있다. 이

러한 항균효과를 실시간으로 확인하기 위하여 MRSA 생물막에 대한 라만 분석을 수행하였다. 라만분광법은 세포의 생화학적 변화를 정량적, 비표지 그리고 빠른 모니터링을 할 수 있어 실행되었다. Petrifilm으로 바이오필름의 성장 단계 별 투여한 유제놀과 반코마이신의 효과를 CFU 값으로 확인하였다. MIC 농도의 반코마이신보다 MIC 유제놀이 약 15프로 이상 높은 바이오필름 제거 효과를 확인하였다. MIC의 2배농도인 MBIC 농도의 유제놀은 대조군의 약 50프로 이상의 제거 효과를 생물막 초기단계에서 보여주었다. 이는 라만 분석과 CFU 계산 결과와 일치하였다. 이 결과에 따르면 라만 분광법을 활용하여 생물막 형성을 모니터링하여 신속한 천연물 유래 항균 효과를 탐색 가능할 것으로 보여진다. 앞으로 라만 분광기를 활용한 새로운 천연 항균제의 개발이 가능할 것으로 생각된다.

주요어 : 황색포도상구균, 생물막, 유제놀, Raman spectroscopy, MRSA, real time monitoring

학번 : 2014-31243